International Telecommunication Union

ITU-R

Radiocommunication Sector of ITU

Report ITU-R M.2500-0
(12/2021)

Coexistence between high-speed railway radiocommunication system between train and trackside operating in the frequency bands 92-94 GHz, 94.1-100 GHz and 102-109.5 GHz, and radio astronomy service and Earth exploration-satellite service (EESS) (active) and EESS (passive) services

M Series

Mobile, radiodetermination, amateur and related satellite services

International Telecommunication Union

Foreword

The role of the Radiocommunication Sector is to ensure the rational, equitable, efficient and economical use of the radio-frequency spectrum by all radiocommunication services, including satellite services, and carry out studies without limit of frequency range on the basis of which Recommendations are adopted.

The regulatory and policy functions of the Radiocommunication Sector are performed by World and Regional Radiocommunication Conferences and Radiocommunication Assemblies supported by Study Groups.

Policy on Intellectual Property Right (IPR)

ITU-R policy on IPR is described in the Common Patent Policy for ITU-T/ITU-R/ISO/IEC referenced in Resolution ITU-R 1. Forms to be used for the submission of patent statements and licensing declarations by patent holders are available from http://www.itu.int/ITU-R/go/patents/en where the Guidelines for Implementation of the Common Patent Policy for ITU-T/ITU-R/ISO/IEC and the ITU-R patent information database can also be found.

Series of ITU-R Reports

(Also available online at http://www.itu.int/publ/R-REP/en)

Series	Title
BO	Satellite delivery
BR	Recording for production, archival and play-out; film for television
BS	Broadcasting service (sound)
BT	Broadcasting service (television)
F	Fixed service
M	**Mobile, radiodetermination, amateur and related satellite services**
P	Radiowave propagation
RA	Radio astronomy
RS	Remote sensing systems
S	Fixed-satellite service
SA	Space applications and meteorology
SF	Frequency sharing and coordination between fixed-satellite and fixed service systems
SM	Spectrum management

Note*: This ITU-R Report was approved in English by the Study Group under the procedure detailed in Resolution ITU-R 1.*

Electronic Publication
Geneva, 2022

REPORT ITU-R M.2500-0

Coexistence between high-speed railway radiocommunication system between train and trackside operating in the frequency bands 92-94 GHz, 94.1-100 GHz and 102-109.5 GHz, and radio astronomy service and Earth exploration-satellite service (EESS) (active) and EESS (passive) services

(2021)

TABLE OF CONTENTS

Page

1 Introduction

Condition based maintenance (CBM) can provide mean-time-before-failure (MTBF) independent maintenance and safety train control and operation. However, in order to introduce CBM in high-speed railway systems, contiguous high-capacity wireless links between in-vehicle and ground networks over several Gb/s are required under high-speed movement around 600 km/h. According to Article **5** of the Radio Regulations, the total frequency bandwidth of 15.4 GHz is allocated for mobile services (MSs) in the frequency range 92-109.5 GHz. These MS bands have a potential to support high-capacity signal transmission between in-vehicle and ground networks. Other advantages to use such high frequencies around 100 GHz are that transceivers can be made compact and equipped in high-speed trains, and the pencil beams which suppress the sidelobe level can be utilized between transceivers. However, high-speed railway radiocommunication systems between train and trackside should be deployed to protect the incumbent services operating in the frequency bands 92-94 GHz, 94.1-100 GHz and 102-109.5 GHz, and the adjacent bands. As a first step, this Report intends to provide sharing and compatibility study results between high-speed railway radiocommunication system between train and trackside and the Earth exploration-satellite service (EESS) (active) and EESS (passive) and radio astronomy service (RAS). Additional Reports will be developed to address compatibility with other incumbent services.

2 Scope

This Report provides results of sharing and compatibility studies between high-speed railway radiocommunication system between train and trackside operating in the bands 92-94 GHz, 94.1-100 GHz and 102-109.5 GHz, and EESS (active), EESS (passive) and RAS operating in these or adjacent bands. The results of analyses contained within this report are limited to the RSTT system and deployment described herein. Additional deployments of this system or new systems will require further studies for sharing and compatibility.

3 Related Recommendations and Reports

Recommendation ITU-R F.699	Reference radiation patterns for fixed wireless system antennas for use in coordination studies and interference assessment in the frequency range from 100 MHz to 86 GHz
Recommendation ITU-R P.452	Prediction procedure for the evaluation of interference between stations on the surface of the Earth at frequencies above about 0.1 GHz
Recommendation ITU-R P.1411	Propagation data and prediction methods for the planning of short-range outdoor radiocommunication systems and radio local area networks in the frequency range 300 MHz to 100 GHz
Recommendation ITU-R RA.769	Protection criteria used for radio astronomical measurements
Recommendation ITU-R RA.1513	Levels of data loss to radio astronomy observations and percentage-of-time criteria resulting from degradation by interference for frequency bands allocated to the radio astronomy service on a primary basis
Recommendation ITU-R RS.1166	Performance and interference criteria for active spaceborne sensors
Recommendation ITU-R RS.1813	Reference antenna pattern for passive sensors operating in the Earth exploration-satellite service (passive) to be used in compatibility analyses in the frequency range 1.4-100 GHz

Recommendation ITU-R RS.1861	Typical technical and operational characteristics of Earth exploration-satellite service (passive) systems using allocations between 1.4 and 275 GHz
Recommendation ITU-R RS.2017	Performance and interference criteria for satellite passive remote sensing
Recommendation ITU-R RS.2105	Typical technical and operational characteristics of Earth exploration-satellite service (active) systems using allocations between 432 MHz and 238 GHz
Report ITU-R F.2239	Coexistence between fixed service operating in 71-76 GHz, 81-86 GHz and 92-94 GHz bands and passive services
Report ITU-R M.2418	Description of railway radiocommunication systems between train and trackside (RSTT)
Report ITU-R M.2442	Current and future usage of railway radiocommunication systems between train and trackside (RSTT)

4 List of acronyms and abbreviations

CCDF	Complementary cumulative distribution function
CPR	Cloud profiling radar
FDR	Frequency dependent rejection
LHC	Left hand circular
OOB	Out-of-band
RAU	Radio access UNIT
RFI	Radio frequency interference
RHC	Right hand circular
RSTT	Railway Radiocommunication System between Train and Trackside

5 Summary of coexistence of 100 GHz band RSTT with the EESS (active), EESS (passive) and RAS

Table 1 shows the frequency band which are already allocated for use of mobile services in the frequency range 92-109.5 GHz. In accordance with Article **5** of the Radio Regulations (see Annex), in the adjacent bands of those frequencies all emissions are prohibited in the following bands: 86-92 GHz, 100-102 GHz and 109.5-111.8 GHz. To coexist with EESS (active), EESS (passive) and RAS, the same schemes developed by Report ITU-R F.2239 – Coexistence between fixed service operating in 71-76 GHz, 81-86 GHz and 92-94 GHz bands and passive services, could be used for sharing and compatibility studies of railway radiocommunication systems. The following sharing and compatibility cases should be addressed, as shown in Fig. 1:

1) mobile service stations such as on-board radio equipment and related radio infrastructure located along trackside operating in the band 92-94 GHz with respect to the protection of Earth exploration-satellite service (EESS) stations operating in the adjacent band 86-92 GHz;

2) mobile service stations such as on-board radio equipment and related radio infrastructure located along trackside operating in the bands 94.1-100 GHz and 102-109.5 GHz with

respect to the protection of Earth exploration-satellite service (EESS) stations operating in the adjacent band 100-102 GHz;

3) mobile service stations such as on-board radio equipment and related radio infrastructure located along trackside operating in the band 102-109.5 GHz with respect to the protection of Earth exploration-satellite service (EESS) stations operating in the adjacent band 109.5-111.8 GHz;

4) mobile service stations such as on-board radio equipment and related radio infrastructure located along trackside operating in the bands 92-94 GHz, 94.1-100 GHz and 102-109.5 GHz with respect to the protection of radio astronomy service (RAS) stations operating in the band 86-111.8 GHz;

5) mobile service stations such as on-board radio equipment and related radio infrastructure located along trackside operating in the bands 92-94 GHz and 94.1-100 GHz with respect to the protection of Earth exploration-satellite service (EESS) stations (active) operating in the adjacent band 94-94.1 GHz;

6) Earth exploration-satellite service (EESS) stations (active) operating in the band 94-94.1 GHz with respect to protect mobile service stations such as on-board radio equipment and related radio infrastructure located along trackside operating in the adjacent bands 92-94 GHz and 94.1-100 GHz.

TABLE 1

Frequency bands already allocated for mobile servicers

	92-94 GHz		94.1-100 GHz		102-109.5 GHz	
	MS		MS		MS	
	BW1 = 2 GHz		BW2 = 5.9 GHz		BW3 = 7.5 GHz	

FIGURE 1

Sharing and compatibility schemes for coexistence between mobile services and passive services

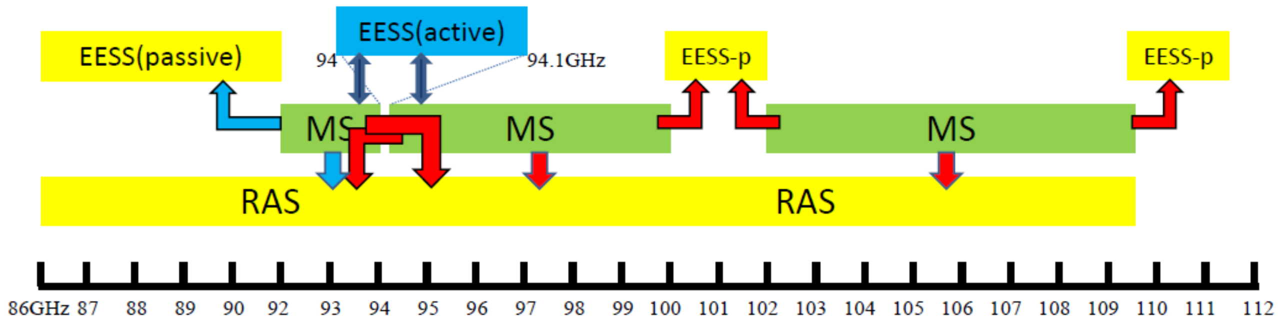

6 System deployment scenarios

6.1 System architecture

Figure 2 shows the schematic concept of 100 GHz wireless connection between on-board equipment and trackside radio access unit. The concept shows that ten trackside radio access units (RAUs) with two antennas are equipped along the railway line. Two on-board transceivers are equipped with the driver's room located at the first car of the train and the conductor's room located at the end car of the train to provide stable communication links between train and trackside. Both on-board transceivers are complementally connected to the trackside radio access units to seamlessly maintain link connection through 100-GHz signals.

FIGURE 2

Concept of 100-GHz wireless connection between on-board and trackside equipment

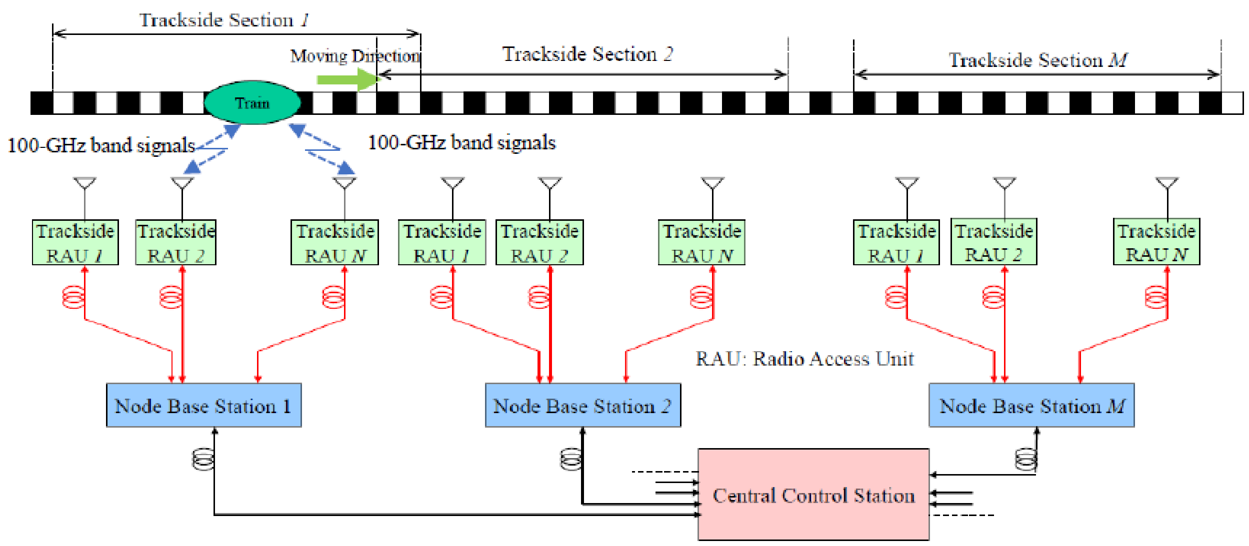

6.2 Linear-cell configuration

Figure 3 illustrates linear-cell configuration of 100-GHz RSTT. The communication zones are formed by the trackside RAUs located along the rail lines. The coverage length of each communication zone is designed in the range 0.5-3 km, depending on the railway line environment such as viaduct, tunnel, cutting, bridge, etc. The same channels are assigned to e.g. communication zones #1 to #N covered by trackside RAUs #1-#N which are connected to node base station through radio over fibre links to transmit/receive high-speed data signals. The communication zones from #1 to #N corresponds to the single frequency network which utilizes frequency channels efficiently. Figure 4 shows the block diagram of node base stations-F/B and trackside RAUs-F/B. The node base station-F transmits/receives multi-channels subcarriers to/from the trackside RAU-F in which no digital signal processing units are equipped and the node base station-B to/from the trackside RAU-B. The four transceivers for forward and backward links are equipped at the same trackside RAU location.

FIGURE 3

Illustration of linear-cell configuration of 100-GHz RSTT

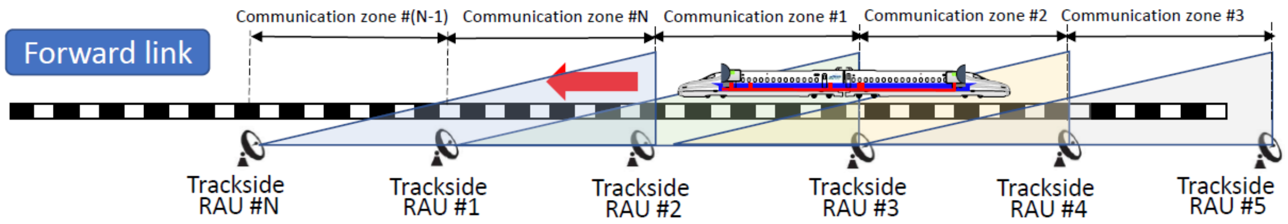

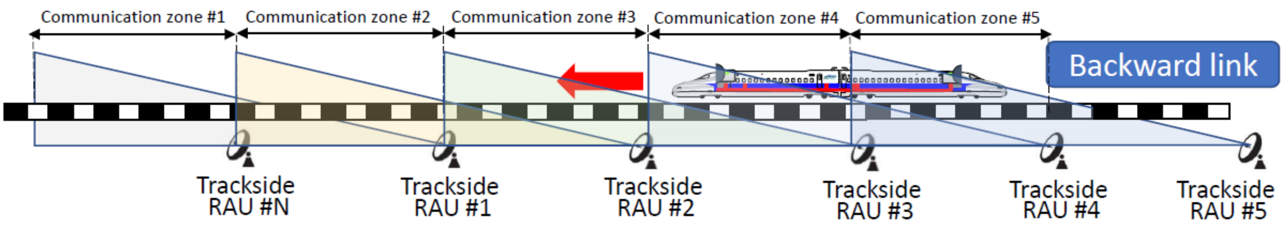

FIGURE 4

Block diagram of node base station and trackside RAU

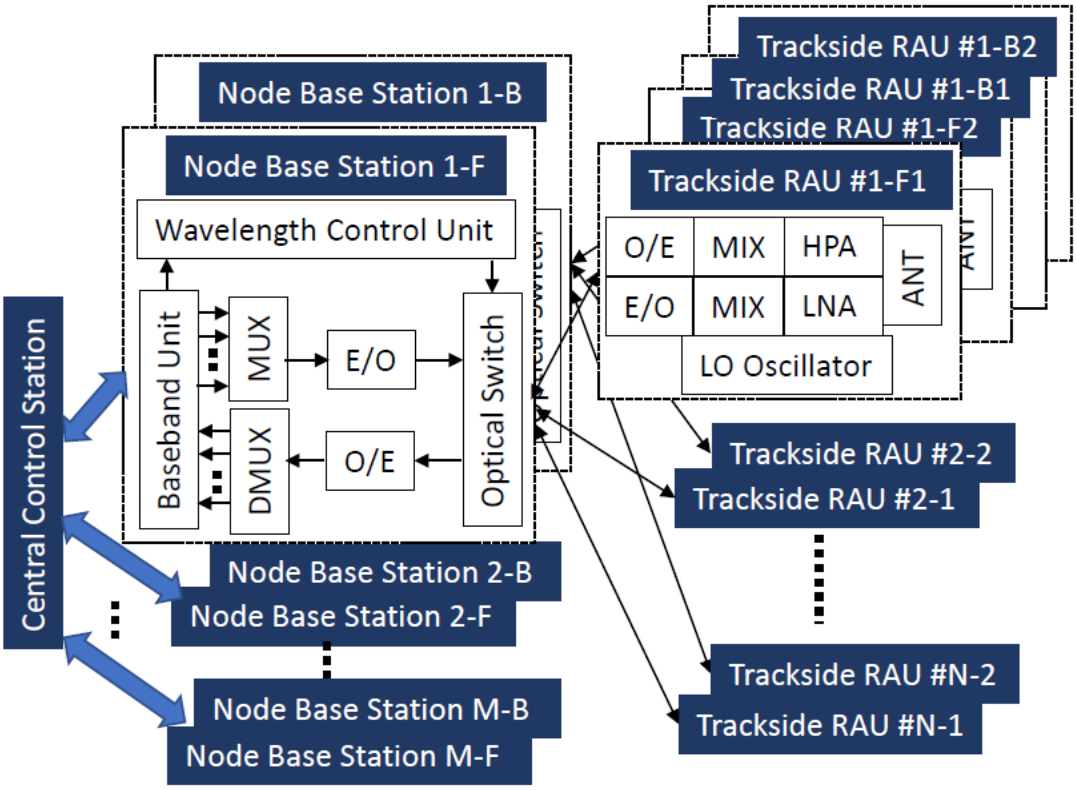

6.3 Number of on-board transceivers

Since two on-board transceivers are equipped with the driver's room located at the first train vehicle and the conductor's room located at the last train vehicle, the total number of on-board transceivers on super express train set in Japan Railway will be four. The number of train set of daily operated super express trains in all Japan Railway companies is shown in Fig. 5. The maximum train set of 230 is observed in the evening of 19:00-20:00 hour. Then the total number of on-board transceivers which are operated in 19:00-20:00 hour becomes 920. This number may be used for sharing and compatibility studies taking into account the coverage area of satellite antennas.

FIGURE 5

Total number of super express train set per one day

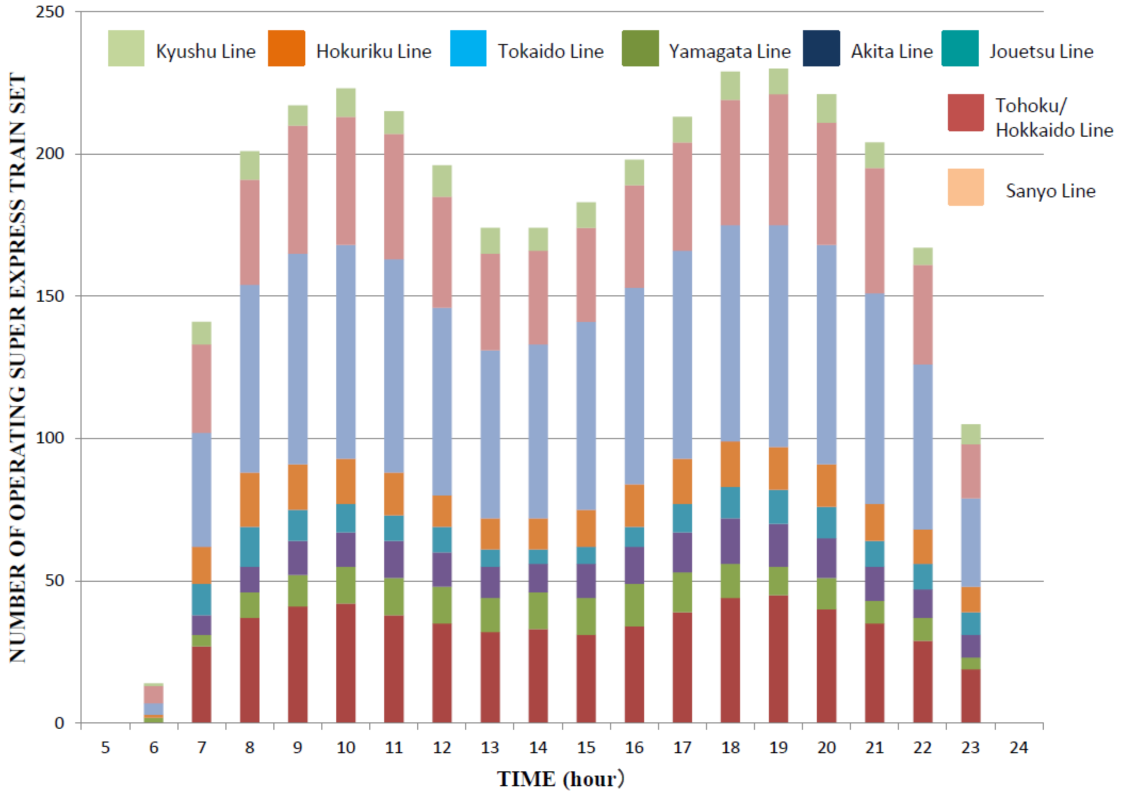

6.4 Number of trackside radio access unit

Figure 6 shows the currently operated super express service lines in Japan Railway companies. Table 2 summarizes the super express service line length and maximum speed of each Japan Railway company. The distance between on-board transceivers and trackside RAUs are changed in the range of 0.5 to 3 km in the condition of operational environment. In the estimation of the number of trackside RAUs, the trackside RAU is equipped 1 km interval along the super express service line. Table 2 also estimated the number of trackside RAUs. One trackside RAU has four transceivers which are independently connected to four on-board transceivers equipped on the super express train set, as described in § 6.2.

FIGURE 6

Map of super express service lines in Japan

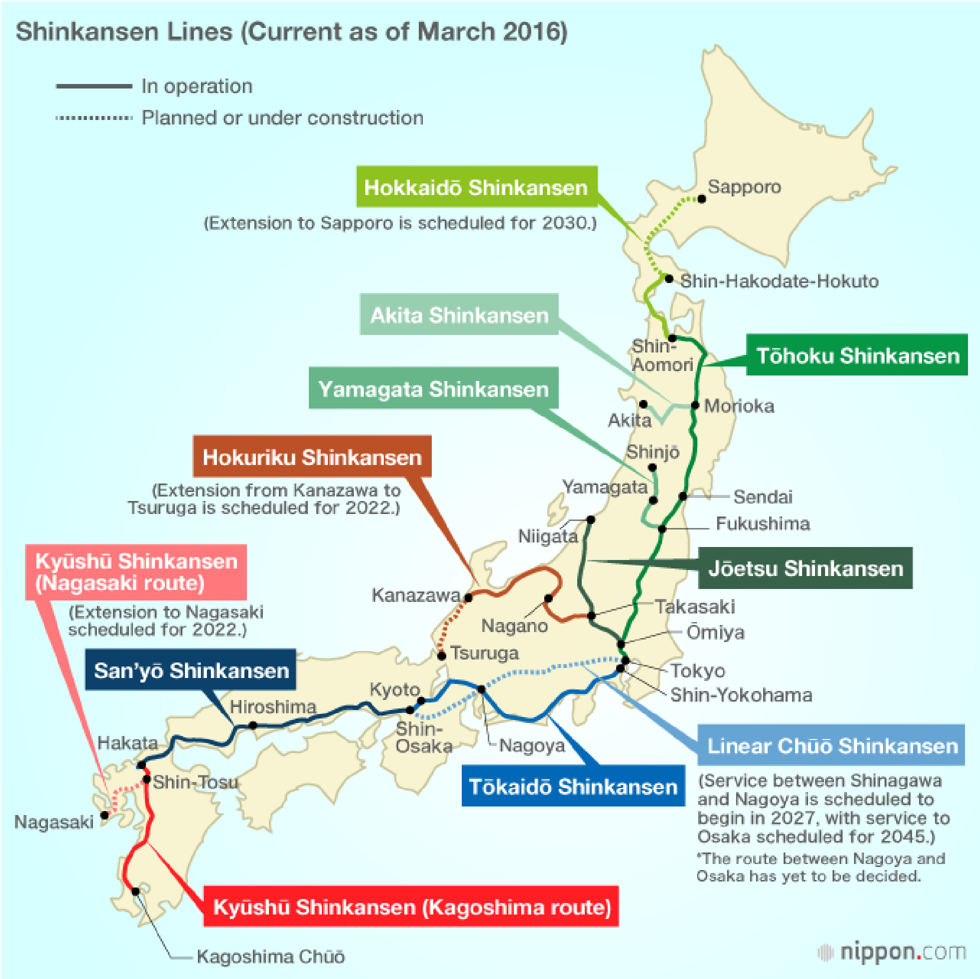

TABLE 2

Estimated number of trackside RAU in each super express service line in Japan

Name of super express line	Service area	Line length (km)	Maximum speed (km/hour)	Estimated number of transceivers	Total tunnel length (km)
Tokaido line	Tokyo – Shin Osaka	562.6	285	2 248	68.663
Sanyo line	Shin Osaka – Hakata	644.0	300	2 576	280.492
Tohoku line	Tokyo – Shin Aomori	713.7	320	2 852	236.0
Hokkaido line	Shin Aomori – Shin Hakodatehokuto	148.8	260	592	94.48
Yamagata line (1)	Fukushima – Shinjo	148.6	130	592	–
Akita line[1]	Morioka – Akita	127.3	130	508	–
Jouetsu line	Tokyo – Niigata	333.9	240	1 332	106.789
Hokuriku line	Tokyo – Kanazawa	450.5	260	1 800	97.289
Kyushu line	Hakata – Kagoshimachuou	288.9	260	1 152	125.021

(1) Yamagata and Akita lines are not included in super express service line, but the same train vehicles are operated in those lines.

6.5 Estimation of RSTT link density

The highest RSTT link density can be expected at the centre area of Tokyo because Tokaido line, Tohoku line, Yamagata line, Akita line, Jouetsu line and Hokuriku line are terminated at Tokyo station. RSTT link density is defined as a ratio of the total number of super express trains in operation and the service railway distance between Shin-Yokohama and Omiya Stations. The RSTT link density and the activated transceivers density in urban area can be estimated to 0.316 vehicle/km and 2.53 transceivers/km from Table 3. This number may be used for sharing and compatibility studies as the worst-case scenario.

TABLE 3

Estimated number of super express trains operating between Shin-Yokohama and Omiya stations

Station	Distance from Tokyo (km)	Estimated number of vehicles in operation [(1)]	Number of activated transceivers
Shin-Yokohama	28.8	7	56
Shinagawa	6.8	3	24
Tokyo	0	0	0
Ueno	3.6	4	32
Omiya	30.3	8	64

(1) This number is estimated by adding all vehicles operating in Tokaido line, Tohoku line, Yamagata line, Akita line, Jouetsu line and Hokuriku line at the time around 19:30 when is the busiest time for business trip.

Figure 7 shows the location of stations and super express service lines in Tokyo area where the highest RSTT link density is estimated. The super express trains are distributed between each station in the hour when the peak train numbers are operated. This area provides the worst-case interference scenario to any active and passive service applications.

FIGURE 7

Super express service lines and stations around Tokyo area

In rural area, the RSTT link density can be estimated in the condition that fifteen super express trains with a maximum speed of 285 km/hour can run on the same service line simultaneously within one hour. The distance between each train set becomes about 20.3 km. The RSTT link density and the activated transceivers density in rural area can be estimated to be 0.05 vehicle/km and 0.39 transceivers/km. In suburban area, the super express train decreases the speed and the average speed is around 180 km/hour. The RSTT link density and the activated transceivers density in suburban area can be estimated to be 0.078 vehicle/km and 0.62 transceivers/km. Table 4 summarizes the estimated RSTT and activated transceiver densities.

TABLE 4

Estimated RSTT link and activated transceivers density in urban, suburban and rural areas

Area	RSTT link density (Vehicle/km)	Activated transceivers density (Transceiver/km)
Urban	0.316	2.53
Suburban	0.078	0.62
Rural	0.049	0.39

6.6 Antenna elevation of on-board transceivers

Table 5 summarizes the operational environment of super-express service lines. Since the maximum gradient of track is 35‰, ±2-degrees of additional antenna elevation of on-board unit and trackside RAU where maximum antenna gain deviation is estimated to be 5 dB from Annex 1 should be taken into account when sharing and compatibility studies are conducted. The average antenna gain of −15 dBi at zenith direction may be used for sharing study.

TABLE 5

Operational environment of super express service line

Parameters	Values
Roadbed width	Typ. 12 m
Vehicle width	Max. 3.4 m
Vehicle height	Max. 4.5 m
Minimum radius of curve	Typ. 4 000 m
Minimum vertical radius of curve	Typ. 10 000 m
Maximum gradient of track	35‰(1)
Maximum superelevation of track	200 mm @ rail gauge (1 435 mm)

(1) The unit ‰ is pronounced as per mill and 1‰ is 0.001 = 0.1%.

7 System characteristics

7.1 System characteristics of railway radiocommunication system between train and trackside operating in the bands 92-94 GHz, 94.1-100 GHz and 102-109.5 GHz

Table 6 summarizes technical and operational characteristics of RSTT stations operating in 92-94 GHz, 94.1-100 GHz and 102-109.5 GHz bands. The total bandwidth of 15.4 GHz can be used for data transmission between on-board radio equipment and trackside radio access units. The transmission distance of these equipment is designed by the railroad line environment.

TABLE 6

System parameters

Frequency range (GHz)	92-94. 94.1-100, 102-109.5
Seamless connection mechanism	Backward and forward switching method
Channel bandwidth (MHz)	400
Channelization (MHz)	See Fig. 8 and Annex 5
Channel aggregation pattern	See Fig. 9
Antenna type	Cassegrain
Antenna gain (dBi)	42 (RAU), 35 (On-board unit)
Antenna beamwidth (degree)	1 (azimuth and elevation)
Antenna height from rail surface (m)	4 (Maximum)
Polarization	Linear
Antenna pattern	See Annex 1 and Recommendation ITU-R F.699
Average transmitting power (dBm)	10
Average e.i.r.p. (dBm)	54
Receiving noise figure (dB)	<10
Maximum transmission data rate (Gb/s)	5-10 (Stationary), 1 (Running)
Maximum transmission distance (km)	0.5-1 (Open), 3 (Tunnel)
Modulation	PSK, QPSK, 16-QAM, 64-QAM
Multiplexing method	FDD/TDD
Maximum running speed (km/h)	600
Wired interface of trackside radio access unit	Recommendation ITU-T G.9803
Propagation model between train and trackside	Recommendation ITU-R P.1411
I/N (dB)	−6

Figure 8 shows the channel arrangement of 100-GHz RSTT which is categorized into three groups. Each group has guard bands at both ends of frequency bands to avoid frequency interferences to the existing radiocommunication services (see Annex 5). Figure 9 shows two channel aggregation pattern which is based on minimum Nyquist bandwidth of 250 MHz and roll-off rate of 0.25. This pattern can ideally transmit 0.5 Gb/s when QPSK modulation technique with a symbol rate of 250 Mb/s is used. Since the maximum data rate per channel is 2 Gb/s when 64 QAM modulation technique is applied, the 8 Gb/s data transmission is feasible by 4-channel bonding pattern.

Figure 10 shows spectrum mask of QPSK modulated 4-channel bonding pattern at RF band. Channels 6, 7, 8 and 9, whose centre frequencies are indicated in Annex 5, are used for 4-channel QPSK modulated signal transmission. The resolution bandwidth of 3 MHz is used for spectrum measurement. The output power per channel P_o is estimated using the following equation:

$$P_o = P_m + 10 \log (OBW/RBW) \qquad (1)$$

where:

P : measured transmitting power (dBm)

OBW : occupied bandwidth (MHz)

RBW : resolution bandwidth (MHz).

Since the measured transmitting power of each channel is about –10.5 dBm, –12 dBm, –12 dBm and –12.5 dBm, the output power of each channel estimated to be 9.7 dBm, 8.2 dBm, 8.2 dBm and 7.7 dBm which are lower than the specification shown in Table 6 due to excess losses between the transmitter and the antenna. Although no spectrum mask of channel 4 or channel 5 is measured, the in-band emission level of channel 4 and channel 5 at the band of 94-94.1 GHz could be estimated from the measured data of the bands of 96.7-96.8 GHz and 94.4-94.5 GHz. They are about –38 dBm/3 MHz and –41 dBm/3 MHz, respectively. Since the bandwidth of the satellite (CPR-L1) is 0.36 MHz, the in-band emission power is estimated to be –47 dBm/0.36 MHz and –51 dBm/0.36 MHz, respectively. The total in-band emission power could be –45.5 dBm/0.36 MHz.

The out-of-band emission level of 100-GHz RSTT is also estimated from the measured spectrum in Fig. 10. It could be about –40 dBm/3 MHz at 92 GHz and then –45 dBm/3 MHz at 89.5 GHz. The level of –45 dBm is the limit value of the measurement system, but this value may provide the worst-case power level of the out-of-band emission. Since the bandwidth of the satellite (L8) is 3 GHz, the total out-of-band emission power in the band of 3 GHz is estimated to be –12.7 dBm.

FIGURE 8

Channel arrangement of 100-GHz RSTT

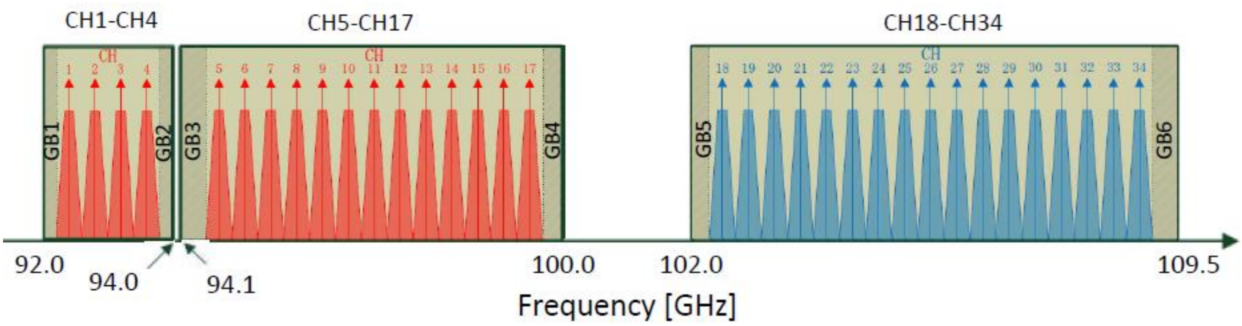

FIGURE 9

Channel aggregation pattern

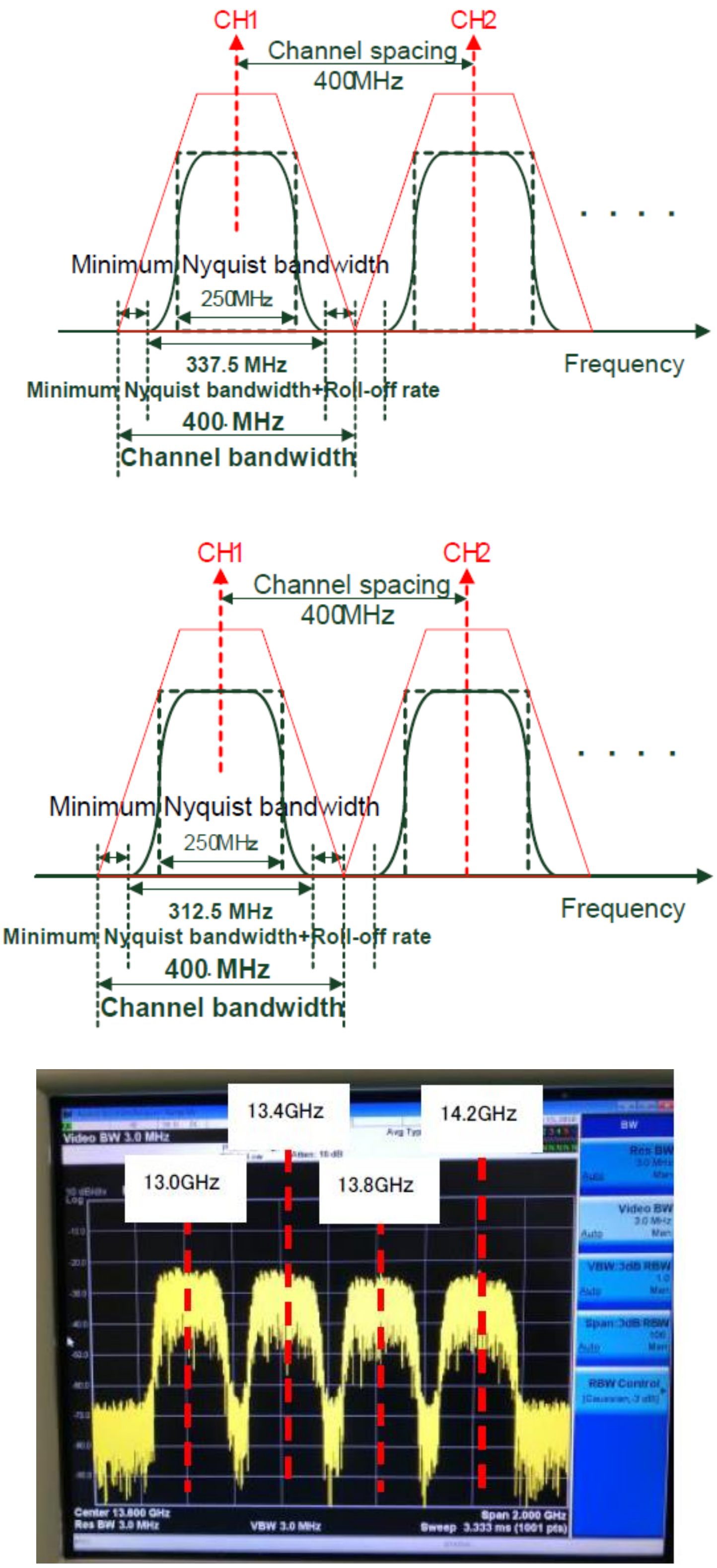

FIGURE 10

Spectrum mask of QPSK modulated 4 channels bonding pattern whose channel number is No. 6 (95.1 GHz), No. 7 (95.5 GHz), No. 8 (95.9 GHz) and No. 9 (96.3 GHz) (see Table 24)

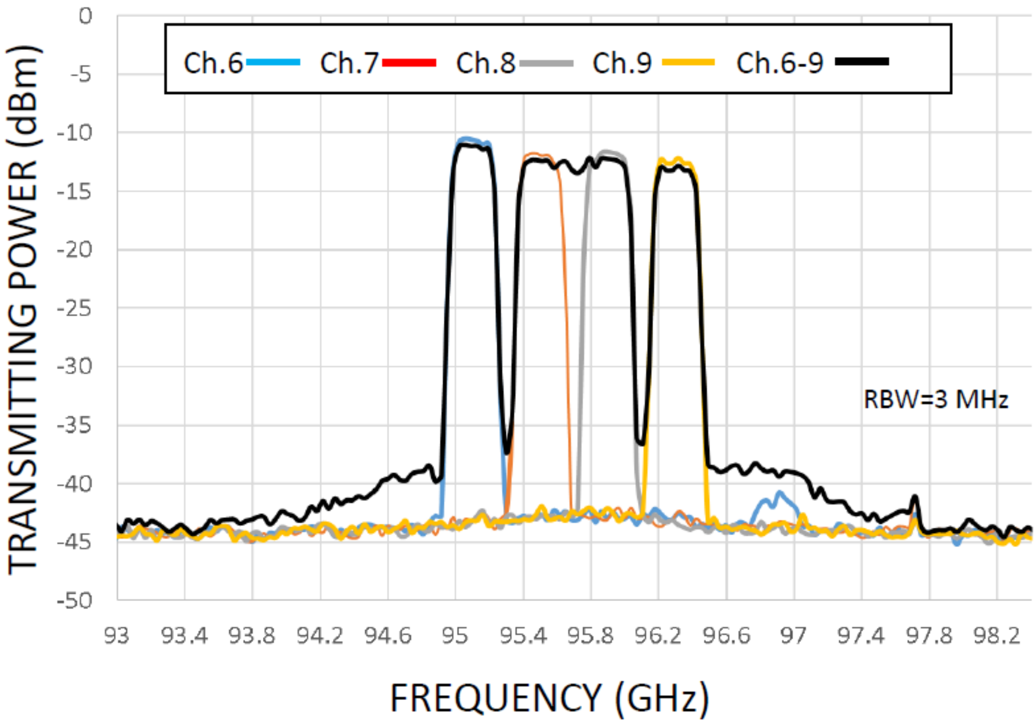

7.2 System characteristics of Earth exploration-satellite service (passive) operating in the frequency range 86-92 GHz

Technical characteristics of spaceborne radiometers in the frequency band of 86-92 GHz are provided in Recommendation ITU-R RS.1861 – Typical technical and operational characteristics of Earth exploration-satellite service (passive) systems using allocations between 1.4 and 275 GHz. The technical characteristics of spaceborne radiometer systems L8 and L5 are presented below in Table 7.

Performance requirements for spaceborne passive sensors in the EESS (passive) are provided by Recommendation ITU-R RS.2017 – Performance and interference criteria for satellite passive remote sensing. The performance criteria for the EESS (passive) radiometers specifies a temperature differential, ΔT_e of 0.05 K and data availability criteria of at least 99.99%.

TABLE 7

Characteristics of EESS (passive) missions in the 86-92 GHz band

	Sensor L5	**Sensor L8**
Sensor type	Mechanical nadir scan	Conical scan
Orbit parameters		
Altitude (km)	822	700
Inclination (degree)	98.7	98.2
Eccentricity	0.001	0.002
Repeat period (days)	29	16
Sensor antenna parameters		
Number of beams	1 beam (steerable in 90 earth fields per scan period)	2
Reflector diameter (m)	0.22	2
Maximum beam gain (dBi)	44.8	62.4
Polarization	H,V	H, V
–3 dB beamwidth	1.1°	0.15°
Instantaneous field of view	Nadir FOV: 16 km (1.1°)	A: 5.1 km × 2.9 km
	Outer FOV: 53 × 27 km*	B: 5.0 km × 2.9 km
Main beam efficiency	95%	91%
Sensor antenna parameters (*cont.*)		
Off-nadir pointing angle (degree)	±49.4	47.5
Beam dynamics	8/3 s scan period	40 rpm
Incidence angle at Earth (degree)	59 *	55
Swath width (km)	2 193	1 450
Cold calibration antenna gain (dBi)	44.8	43.4
Cold calibration angle (degrees re. satellite track)	−90° ± 3.9°	115.5°
Cold calibration angle (degrees re. nadir direction)	(66° to 81°)*	97.0°
Sensor receiver parameters		
Sensor integration time (ms)	18	1.2
Channel bandwidth	2 800 MHz centred at 89 GHz	3 000 MHz centred at 89 GHz
Measurement spatial resolution		
Horizontal resolution (km)	16	2.9
Vertical resolution (km)	16	5.1

NOTE 1 – * Indicates that a particular sensor is flown on different missions, with different orbit and sensor parameters.

7.3 System characteristics of Earth exploration-satellite service (active) operating in the frequency range 94-94.1 GHz

Technical characteristics of cloud profile radars (CPRs) in the frequency band of 94.0-94.1 GHz are given in Recommendation ITU-R RS.2105 – Typical technical and operational characteristics of Earth exploration-satellite service (active) systems using allocations between 432 MHz and 238 GHz. The technical characteristics for two CPR systems CPR-L1 and CPR-L2 are presented below in Table 8.

Performance requirements for spaceborne active sensors in the EESS (active) are given in Recommendation ITU-R RS.1166-4 – Performance and interference criteria for active spaceborne sensors. The performance criteria for the EESS (active) cloud profile radars requires a measurement of a minimum reflectivity of –30 dBz ±10%, *I*/*N* no greater than –10 dB and random data availability criteria of no less than 99.8%.

TABLE 8

Characteristics of EESS (active) missions in the 94-94.1 GHz band

Parameter	CPR-L1	CPR-L2
Sensor type	Cloud Profiling Radar	Cloud Profiling Radar
Type of orbit	SSO	SSO
Altitude (km)	705	393
Inclination (degree)	98.2	97
Ascending Node LST	13:30	10:30 (1)
Repeat period (days)	16	25
Antenna type	Parabolic reflector to Offset Cassegrain antenna	Parabolic reflector
Antenna diameter (m)	1.85-2.5	2.5
Antenna (transmit and receive) peak gain (dBi)	63.1-65.2	65.2
Polarization	linear	LHC, RHC
Incidence angle at Earth (degree)	0	0
Azimuth scan rate (rpm)	0	0
Antenna beam look angle (degree)	0	0
Antenna beam azimuth angle (degree)	0	0
Antenna elevation beamwidth (degree)	0.12	0.095
Antenna azimuth beamwidth (degree)	0.12	0.095
Beam width (degree)	0.095-0.108	0.095
RF centre frequency (MHz)	94.050	94.050
RF bandwidth (MHz)	0.36	7
Transmit Pk power (W)	1 000	1 430
Transmit Ave. power (W)	21.31	28.8
Pulsewidth (μsec)	3.33	3.3
Pulse repetition frequency (PRF) (Hz)	4 300	6 100-7 500
Chirp rate (MHz/μsec)	N/A (2)	2.1
Transmit duty cycle (%)	1.33	2.01
Minimum sensitivity (dBz)	–30 to –35	–30 to –35
Horizontal resolution	0.7-1.9 km	800 m
Vertical resolution (m)	250-500	500
Doppler range	±10 m/s	–10 ~ +10 m/s
Doppler accuracy (m/s)	1	1
System noise figure (dB)	7	7

(1) Descending.

(2) The sensor uses an unmodulated pulse.

8 Interference scenarios

The four interference scenarios listed in Table 9 and shown in Fig. 11 are considered between land mobile service applications (RSTT), and EESS (active), EESS (passive) and RAS.

TABLE 9

Interference scenarios

Scenario	Interfering	Interfered with	Propagation model
A-1	RSTT on-board terminal	EESS space station	Free space
A-2	RSTT trackside station	EESS space station	Free space
B-1	RSTT on-board terminal	EESS space station	Free space
B-1	EESS space station	RSTT on-board terminal	Free space
B-2	RSTT trackside station	EESS space station	Free space
B-2	EESS space station	RSTT trackside station	Free space
C-1	RSTT on-board terminal	RAS earth station	P.452-16
C-2	RSTT trackside station	RAS earth station	P.452-16

FIGURE 11

Illustration of interference scenario

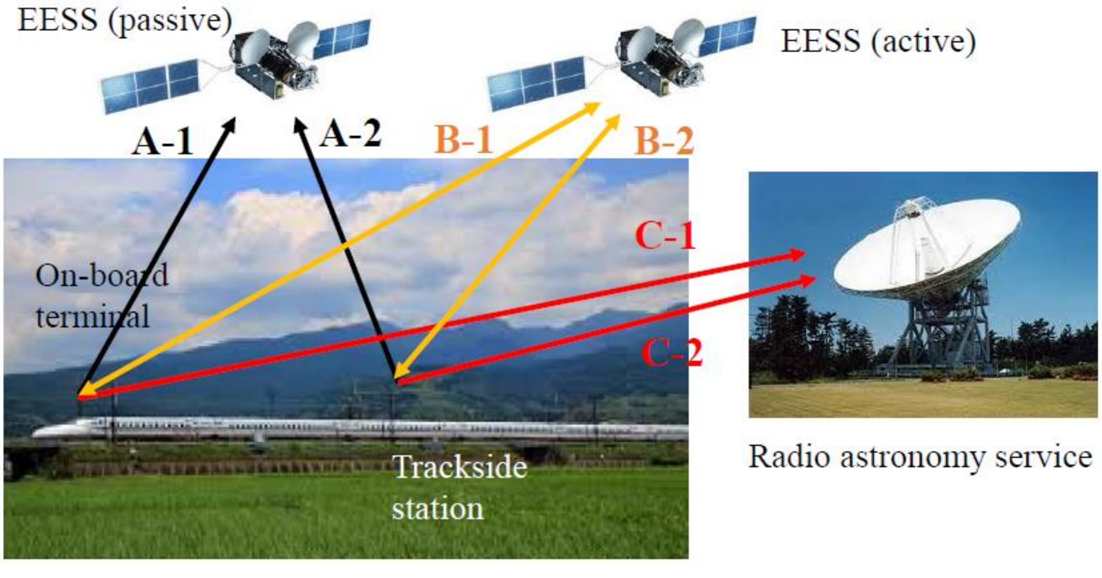

9 Sharing and compatibility studies with EESS (active). EESS (passive) and RAS

9.1 Compatibility studies for Earth exploration-satellite service (active)

Interference criteria for spaceborne active sensors in the EESS (active) are provided by Recommendation ITU-R RS.1166-4 – Performance and interference criteria for active spaceborne sensors. The interference threshold criteria for the EESS (active) Cloud Profile Radars in the 94.0-94.1 GHz frequency band is –155 dBW over 300 kHz. The study results are included in Annex 2.

9.2 Compatibility studies for Earth exploration-satellite service (passive)

Interference requirements for spaceborne passive sensors in the EESS (passive) are given in Recommendation ITU-R RS.2017-0 – Performance and interference criteria for satellite passive remote sensing. The interference threshold criteria for the EESS (passive) radiometer in the 8692 GHz frequency band is –169 dBW with a percentage of area or time permissible interference level may be exceeded of 0.01%. The study results are included in Annex 3.

9.3 Sharing studies for radio astronomy service

Protection criteria for radio astronomy observations are provided by Recommendation ITU-R RA.769-2, with levels of data loss to radio astronomy observations and percentage-of-time criteria resulting from degradation by interference for frequency bands allocated to the radio astronomy service on a primary basis available in Recommendation ITU-R RA.1513. These Recommendations should be used in evaluating compatibility to radio astronomy observatories. Two initial sharing studies are shown in Annex 4. The both initial studies show that the received power level at an RAS antenna may exceed the threshold level in the condition of line-of-sight transmission path. The study results detailing both line-of-sight and terrain-influenced signal levels are shown in Annex 4. Terrain significantly reduces the required separation distances to reach compatibility with RAS in some cases. Generally, radio astronomy sites and RSST may coexist using a combination of separation distance and leveraging terrain, and configuration of the RSST transmitters geometry and power levels.

Annex 1

Measurement results of radiation pattern in the frequency range 92-100 GHz

This Annex provides various antenna radiation pattern for 100 GHz RSTT.

FIGURE 12

Measured radiation pattern of 44-dBi antenna

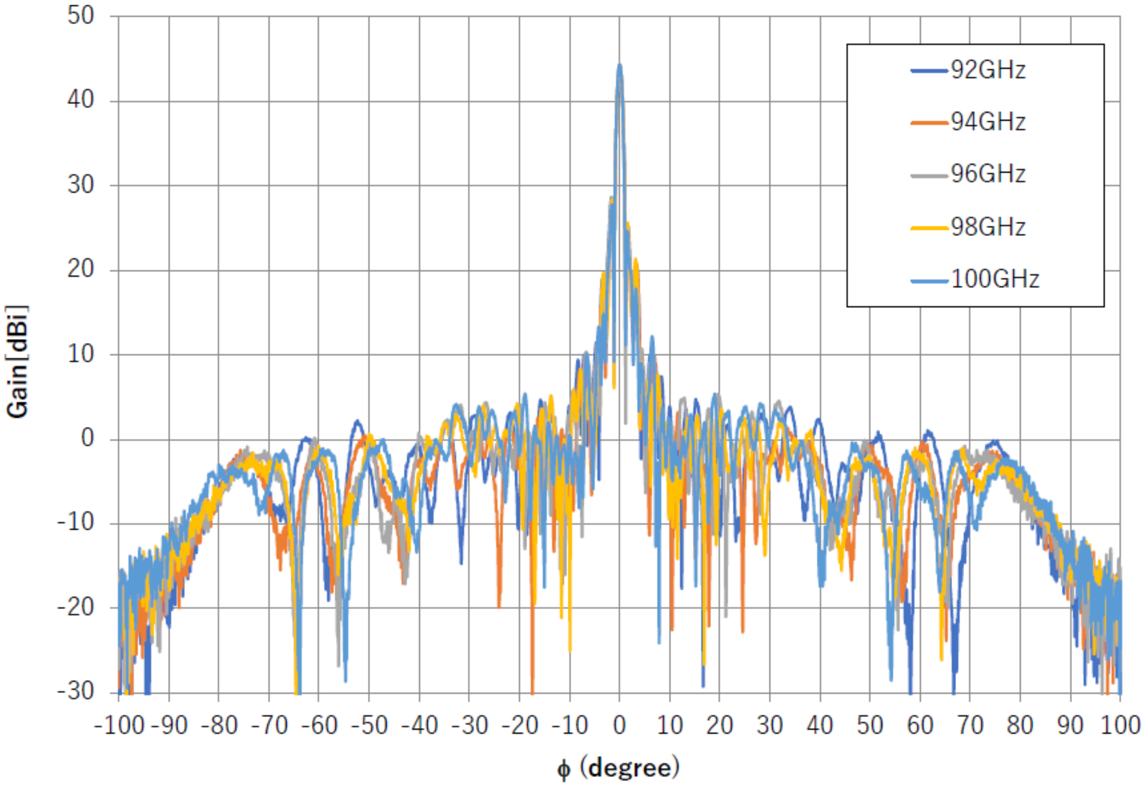

FIGURE 13

Measured radiation pattern of 42-dBi antenna

(a) Off-axis angle from −90 to +90 degrees

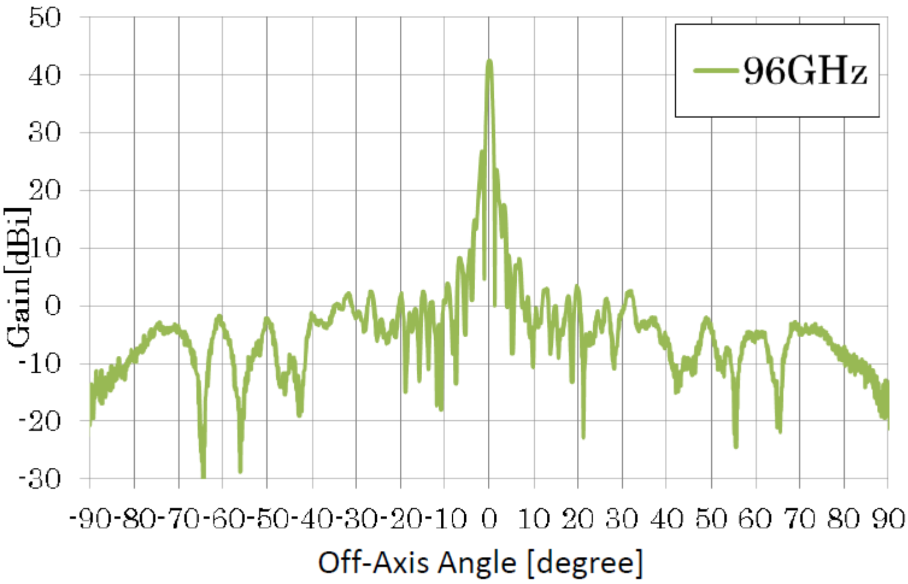

(b) Off-axis angle from −10 to +10 degrees

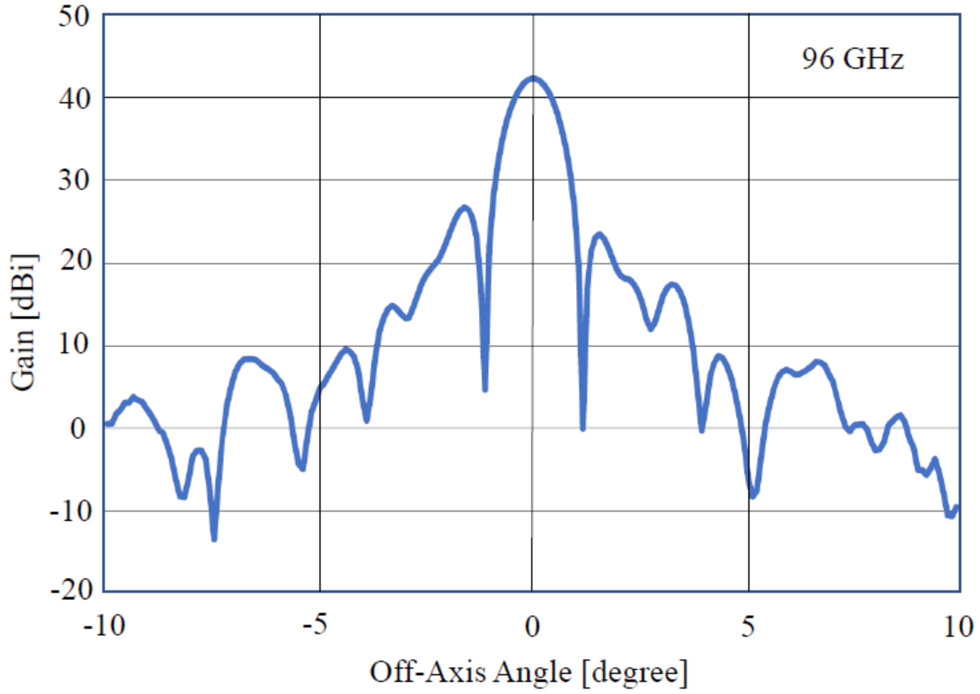

FIGURE 14

Measured radiation pattern of 35-dBi antenna

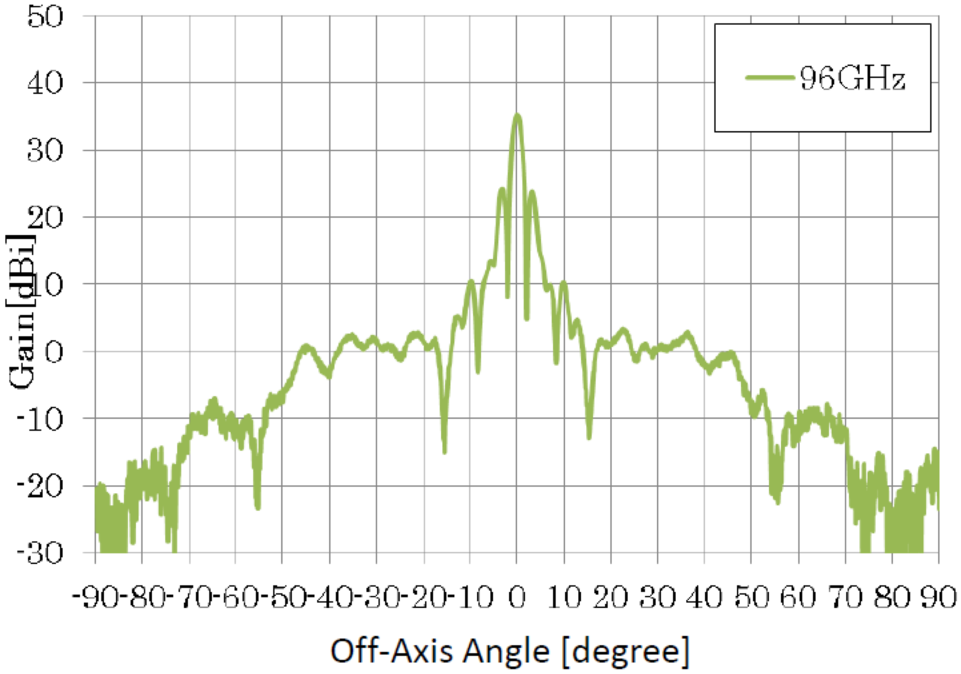

FIGURE 15

External view of trackside RAU

Annex 2

Analysis of potential OOB interference to a spaceborne cloud profile radar in the 94.0-94.1 GHz band from RSTT systems in adjacent bands

1 Introduction

The 94.0-94.1 GHz band is allocated to Earth exploration-satellite service (EESS) (active) on a primary basis for EESS (active) spaceborne active sensors, such as cloud profile radars (CPRs). Herein are presented technical characteristics of two typical EESS (active) cloud profile radar systems operating in the frequency band 94.0-94.1 GHz and technical characteristics for typical Railway Radiocommunication Systems between Train and Trackside (RSTT) stations proposed for adjacent bands 92.0-94.0 GHz and 94.1-96.0 GHz. Performance criteria and interference criteria are provided for active spaceborne cloud profile radar operating in the 94.0-94.1 GHz frequency band. Preliminary calculations are performed to determine the amount of attenuation needed to be applied to railway RSTT systems out-of-band (OOB) emission levels in relation to the RSTT in-band emission levels in order for the out-of-band RSTT emissions to not exceed the EESS (active) interference protection criteria levels.

2 Interference from railway RSTT systems into EESS (active)

For assessing the potential for interference from the railway RSTT systems into EESS (active) systems, three different geometrical scenarios are considered. The first is coupling of the antenna main lobe of a nadir-looking EESS (active) satellite with the sidelobes of the railway RSTT system antenna. The second geometrical scenario is coupling of the sidelobes of both the EESS (active) sensor antenna and the railway RSTT system antenna and the third geometrical scenario is coupling between the mainbeam of the railway RSTT system antenna and the EESS (active) sensor antenna sidelobes occurring when the EESS (active) satellite is on the horizon with respect to the railway RSTT system.

The peak interfering signal power level, I (dBW), received by a spaceborne radar from a terrestrial source is calculated from

$$I = 10 \log P_t + G_t + G_r - (32.44 + 20 \log (f R)) - L_a \quad \text{(A2-1)}$$

where:

- P_t : peak terrestrial source transmitter power (W)
- G_t : terrestrial source antenna gain towards spaceborne sensor (dBi)
- G_r : spaceborne radar antenna gain towards terrestrial source (dBi)
- f : frequency (MHz)
- R : slant range between spaceborne sensor and terrestrial source (km)
- L_a : attenuation due to atmospheric absorption (dB).

Attenuation due to atmospheric absorption, L_a, is dependent upon the path length to the satellite through the Earth's atmosphere, and hence upon the elevation angle from the terrestrial source to the satellite. At frequencies around 94 GHz, L_a decreases rapidly from about 100 dB at 0° elevation angles to 1.5 dB at 90° elevation angles. L_a is not included in the following tables of calculation of the interference levels and margins.

The interference due to mainlobe reception of the CPR antenna from the RSTT sidelobes allows for the highest values of RFI levels of the three geometrical scenarios. For CPR-L1 and CPR-L2, the CPR-L1 system is impacted the most by interference due to its narrower receiver bandwidth of 300 kHz.

For geometric scenario 1 for coupling between the CPR-L1 mainlobe and the railway RSTT sidelobes (elevation angle at 90°), preliminary calculations are provided in Tables 10 (Case 1) and 11 (Case 2) which indicate the amount of attenuation with regard to the in-band power emission level of the railway RSTT system needed to be applied to railway RSTT systems OOB emissions in order for them to meet the EESS (active) interference protection criteria.

Considering CPR-L1, two cases were analysed where the railway RSTT antenna gain in the sidelobes was –10 dBi and 14 dBi, and the density of railway RSTT systems was 10 and 100 in the CPR footprint. The EESS active noise figure used is 7 dB which results in the interference protection criteria threshold of −153.2 dBW. The calculated attenuations in regard to the in-band power emission level of the railway RSTT system needed to meet the EESS (active) interference protection criteria are 9.5 dB in Case 1 to 43.5 dB in Case 2.

For geometric scenario 2 for coupling between the CPR-L1 sidelobes and the railway RSTT sidelobes (elevation angle at 45 degrees), preliminary calculations of two Cases examined are provided in Tables 12 (Case 1) and 13 (Case 2) which indicate the amount of attenuation in regard to the in-band power emission level of the railway RSTT system emissions in order that they meet the EESS (active) interference protection criteria for CPR-L1. The two cases were examined with the railway RSTT system antenna gain in the sidelobes at 0 dBi and 14 dBi, and the density of railway RSTT systems set at 10 and 100 in the CPR footprint, respectively. The EESS (active) system noise figure was 7 dB which resulted in the interference protection criteria threshold of –153.2 dBW. The calculations show that the EESS (active) interference criteria are met with margins of 58.1 dB for Case 1 and 34.1 dB for Case 2.

For geometric scenario 3 for coupling between the CPR-L1 sidelobes and the railway RSTT mainlobe (elevation angle at 0 degree), preliminary calculations of two Cases examined are provided in Tables 14 (Case 1) and 15 (Case 2) which indicate the amount of attenuation with regard to the in-band power emission level of the railway RSTT system emissions in order that they meet the EESS (active) interference protection criteria for CPR-L1. The two cases were examined with the railway RSTT system antenna gain in the mainlobe at 44 dBi, and the density of railway RSTT systems set at 10 and 100 in the CPR footprint, respectively. The EESS active system noise figure was 7 dB which resulted in the interference protection criteria threshold of –153.2 dBW. The calculations show that the EESS (active) interference criteria are met with margins of 24.3 dB for Case 1 and 14.3 dB for Case 2.

TABLE 10

RFI from railway RSTT into EESS (active) at 94 GHz (Case 1)
First Geometric Scenario: CPR M/L to RSTT S/L

Case 1: Calculation of receiving power at 90-degree elevation (G_t = −10 dBi, 10 railway RSTTs in beam)		
	CPR-L1	
	Value	**dB**
RSTT transmit power (W)	0.01	–20.00
Gain_xmit (dBi)		–10.00
e.i.r.p. (dBW)		–30.00
Gain_rcv (dBi)		65.20
$1/R^2$ (km)	705	–56.96
$1/f^2$ (MHz)	94 050	–99.47
L-prop (dB)		–188.87
No. of RSTTs in beam	10	10.00
Interference power (dBW)		–143.67
k	1.38E-23	–228.60
Temperature (K)	290	24.62
BW_EESS (MHz)	0.3	54.77
NF_EESS (dB)		7.00
Noise power (dBW)		–143.17
I/N (dB)		–0.50
I/N criteria (dB)		–10.00
Margin (dB) (attenuation)		–9.50

TABLE 11

**RFI from railway RSTT into EESS (active) at 94 GHz (Case 2)
First Geometric Scenario: CPR M/L to RSTT S/L**

Case 2: Calculation of receiving power at 90-degree elevation (G_t = 14 dBi, 100 railway RSTTs in beam)		
	CPR–L1	
	Value	**dB**
RSTT transmit power (W)	0.01	–20.00
Gain_xmit (dBi)		14.00
e.i.r.p. (dBW)		–6.00
Gain_rcv (dBi)		65.20
$1/R^2$ (km)	705	–56.96
$1/f^2$ (MHz)	94 050	–99.47
L-prop (dB)		–188.87
No. of RSTTs in beam	100	20.00
Interference power (dBW)		–109.67
k	1.38E–23	–228.60
Temperature (K)	290	24.62
BW_EESS (MHz)	0.3	54.77
NF_EESS (dB)		7.00
Noise power (dBW)		–143.17
I/N (dB)		33.50
I/N criteria (dB)		–10.00
Margin (dB) (attenuation)		–43.50

TABLE 12

**RFI from railway RSTT into EESS (active) at 94 GHz (Case 1)
Second Geometric Scenario: CPR S/L to RSTT S/L**

Case 1: Calculation of receiving power at 45-degree elevation (G_t = 0 dBi, 10 railway RSTTs in beam)		
	CPR-L1	
	Value	**dB**
RSTT transmit power (W)	0.01	–20.00
Gain_xmit (dBi)		0.00
e.i.r.p. (dBW)		–20.00
Gain_rcv (dBi)		–9.80
$1/R^2$ (km)	952	–59.57
$1/f^2$ (MHz)	94 050	–99.47
L-prop (dB)		–191.48
No. of RSTTs in beam	10	10.00
Interference power (dBW)		–211.28

TABLE 12 (*end*)

Case 1: Calculation of receiving power at 45-degree elevation (G_t = 0 dBi, 10 railway RSTTs in beam)		
	CPR-L1	
	Value	**dB**
k	1.38E-23	–228.60
Temperature (K)	290	24.62
BW_EESS (MHz)	0.3	54.77
NF_EESS (dB)		7.00
Noise power (dBW)		–143.17
I/*N* (dB)		–68.11
I/*N* criteria (dB)		–10.00
Margin (dB) (attenuation)		58.11

TABLE 13

RFI from railway RSTT into EESS (active) at 94 GHz (Case 2)
Second Geometric Scenario: CPR S/L to RSTT S/L

Case 2: Calculation of receiving power at 45-degree elevation (G_t=14 dBi, 100 railway RSTTs in beam)		
	CPR-L1	
	Value	**dB**
RSTT transmit power (W)	0.01	–20.00
Gain_xmit (dBi)		14.00
e.i.r.p. (dBW)		–6.00
Gain_rcv (dBi)		–9.80
$1/R^2$ (km)	952	–59.57
$1/f^2$ (MHz)	94 050	–99.47
L-prop (dB)		–191.48
No. of RSTTs in beam	100	20.00
Interference power (dBW)		–187.28
k	1.38E-23	–228.60
Temperature (K)	290	24.62
BW_EESS (MHz)	0.3	54.77
NF_EESS (dB)		7.00
Noise power (dBW)		–143.17
I/*N* (dB)		–44.11
I/*N* criteria (dB)		–10.00
Margin (dB) (attenuation)		34.11

TABLE 14

RFI from railway RSTT into EESS (active) at 94 GHz (Case 1)
Third Geometric Scenario: CPR S/L to RSTT M/L

Case 1: Calculation of receiving power at 0-degree elevation (G_t = 44 dBi, 10 railway RSTTs in beam)		
	CPR-L1	
	Value	**dB**
RSTT transmit power (W)	0.01	–20.00
Gain_xmit (dBi)		44.00
e.i.r.p. (dBW)		24.00
Gain_rcv (dBi)		–9.80
$1/R^2$ (km)	3 081	–69.77
$1/f^2$ (MHz)	94 050	–99.47
L-prop (dB)		–201.68
No. of RSTTs in beam	10	10.00
Interference power (dBW)		–177.48
k	1.38E-23	–228.60
Temperature (K)	290	24.62
BW_EESS (MHz)	0.3	54.77
NF_EESS (dB)		7.00
Noise power (dBW)		–143.17
I/*N* (dB)		–34.31
I/*N* criteria (dB)		–10.00
Margin (dB) (attenuation)		24.31

TABLE 15

RFI from railway RSTT into EESS (active) at 94 GHz (Case 2)
Third Geometric Scenario: CPR S/L to RSTT M/L

Case 2: Calculation of receiving power at 0-degree elevation (G_t = 44 dBi, 100 railway RSTTs in beam)		
	CPR-L1	
	Value	**dB**
RSTT transmit power (W)	0.01	–20.00
Gain_xmit (dBi)		44.00
e.i.r.p. (dBW)		24.00
Gain_rcv (dBi)		–9.80
$1/R^2$ (km)	3 081	–69.77
$1/f^2$ (MHz)	94 050	–99.47
L-prop (dB)		–201.68
No. of RSTTs in beam	100	20.00
Interference power (dBW)		–167.48

TABLE 15 (*end*)

Case 2: Calculation of receiving power at 0-degree elevation (G_t = 44 dBi, 100 railway RSTTs in beam)		
	CPR-L1	
	Value	**dB**
k	1.38E-23	–228.60
Temperature (K)	290	24.62
BW_EESS (MHz)	0.3	54.77
NF_EESS (dB)		7.00
Noise power (dBW)		–143.17
I/*N* (dB)		–24.31
I/*N* criteria (dB)		–10.00
Margin (dB) (attenuation)		14.31

3 Summary

For the three different geometrical interaction scenarios described involving antenna beam coupling between railway RSTT systems and CPRs, the RFI levels at the CPR are highest for the geometrical situation of coupling between the nadir-looking CPR antenna and the sidelobes of the railway RSTT system antenna. With the second geometrical scenario where there is coupling of the sidelobes of both the CPR antenna and the railway RSTT system antenna; the RFI levels are lower than for the first geometric scenario. In the third geometrical scenario where coupling between the mainbeam of the railway RSTT system antenna and the CPR antenna sidelobes with the CPR satellite on the horizon with respect to the railway RSTT systems occurs, the interference was lower than the first geometric scenario as well. The CPR-L1 with the narrower receiver bandwidth of 300 kHz, is more sensitive than is CPR-L2. Two cases of railway RSTT deployment and their interference impact to CPR-L1 were analysed to arrive at a preliminary calculation of attenuation in regard to in-band emission levels of railway RSTT systems required to meet the Rec. ITU-R RS.1166-4 protection criteria for CPR-L1. The two cases consider the railway RSTT antenna gain in the sidelobes at the level in Fig. 2 for the appropriate elevation angle and a higher level estimated due to irregularities in the trainside area, and the density of railway RSTT systems at 10 and 100 in the footprint of the CPR-L1 sensor. For the first geometric scenario, in order to meet the EESS (active) Recommendation ITU-R RS.1166-4 protection criteria for CPR-L1, railway RSTT system in-band emission levels would have to be attenuated 9.5 dB when considering Case 1 and 43.5 dB when considering Case 2 at the band edges adjoining the EESS (active) band 94.0-94.1 GHz.

Annex 3

Analysis of potential OOB interference to a spaceborne radiometer in the 86.0-92.0 GHz band from RSTT systems in adjacent bands

1 Introduction

The 86.0-92.0 GHz band is allocated to Earth exploration-satellite service (EESS) (passive) on a primary basis for EESS (passive) spaceborne passive sensors, such as spaceborne radiometers. Herein are presented technical characteristics of one typical EESS (passive) radiometer system operating in the frequency band 86.0-92.0 GHz and technical characteristics for typical Railway Radiocommunication Systems between Train and Trackside (RSTT) stations proposed for adjacent band 92.0-94.0 GHz. Performance criteria and interference criteria are provided for passive spaceborne radiometers operating in the 86.0-92.0 GHz frequency band. Preliminary calculations are performed to determine the amount of attenuation needed to be applied to railway RSTT systems out-of-band (OOB) emission levels in relation to the RSTT in-band emission levels in order for the out-of-band RSTT emissions to not exceed the EESS (passive) interference protection criteria levels.

The compatibility study is performed in response to World Radio Conference 2019 (WRC-19) agenda item 1.11, Resolution **236 (WRC-15)**, which addresses the need for harmonized frequency bands for use by railway RSTT.

2 Interference from railway RSTT systems into EESS (passive)

2.1 Static analysis based on interference with specific geometric scenarios

For assessing the potential for interference from the railway RSTT systems into EESS (passive) systems, three different geometrical scenarios are considered. The first is coupling of the antenna main lobe of a conically scanning antenna of an EESS (passive) satellite with the sidelobes of the railway RSTT system antenna. The second geometrical scenario is coupling of the sidelobes of both the EESS (passive) sensor antenna and the railway RSTT system antenna and the third geometrical scenario is coupling between the mainbeam of the railway RSTT system antenna and the EESS (passive) sensor antenna sidelobes occurring when the EESS (passive) satellite is on the horizon with respect to the railway RSTT system.

The peak interfering signal power level, I (dBW), received by a spaceborne radiometer from a terrestrial source is calculated from

$$I = 10 \log P_t + G_t + G_r - (32.44 + 20 \log (f R)) - L_a \qquad \text{(A3-1)}$$

where:

- P_t: peak terrestrial source transmitter power (W)
- G_t: terrestrial source antenna gain towards spaceborne sensor (dBi)
- G_r: spaceborne radiometer antenna gain towards terrestrial source (dBi)
- f: frequency (MHz)
- R: slant range between spaceborne sensor and terrestrial source (km)
- L_a: attenuation due to atmospheric absorption (dB).

Attenuation due to atmospheric absorption, L_a, is dependent upon the path length to the satellite through the Earth's atmosphere, and hence upon the elevation angle from the terrestrial source to the satellite. At frequencies around 92 GHz, L_a decreases rapidly from about 100 dB at 0-degree elevation angles to 1.5 dB at 90 degrees elevation angles. L_a is not included in Tables 16 to 21 of calculation of the interference levels and margins.

The interference due to mainlobe reception of the radiometer L-8 antenna from the RSTT sidelobes allows for the highest values of RFI levels of the three geometrical scenarios. For geometric scenario 1 for coupling between the radiometer L-8 mainlobe and the railway RSTT sidelobes (elevation angle at 55 degrees), preliminary calculations are provided in Tables 16 (Case 1) and 17 (Case 2) which indicate the amount of attenuation in regard to the in-band power emission level of the railway RSTT system needed to be applied to railway RSTT systems OOB emissions in order for them to meet the EESS (passive) interference protection criteria. Considering radiometer L-8, two cases were analysed where the railway RSTT antenna gain in the sidelobes was 0 dBi and 14 dBi, and the density of railway RSTT systems was 10 and 100 in the CPR footprint. The EESS passive interference protection criteria threshold is −169.0 dBW. The calculated attenuations in regard to the in-band power emission level of the railway RSTT system needed to meet the EESS (passive) interference protection criteria are 28.7 dB in Case 1 to 52.7 dB in Case 2.

For geometric scenario 2 for coupling between the radiometer L-8 sidelobes and the railway RSTT sidelobes (elevation angle at 90 degrees), preliminary calculations of two Cases examined are provided in Tables 18 (Case 1) and 19 (Case 2) which indicate the amount of attenuation in regard to the in-band power emission level of the railway RSTT system emissions in order that they meet the EESS (passive) interference protection criteria for radiometer L-8. The two cases were examined with the railway RSTT system antenna gain in the sidelobes at −10 dBi and 14 dBi, and the density of railway RSTT systems set at 10 and 100 in the CPR footprint, respectively. The EESS passive interference protection criteria threshold is −169.0 dBW. The calculations show that the EESS (passive) interference criteria are met with margins of 49.4 dB for Case 1 and 15.4 dB for Case 2.

For geometric scenario 3 for coupling between the radiometer L-8 sidelobes and the railway RSTT mainlobe (elevation angle at 0 degree), preliminary calculations of two Cases examined are provided in Tables 20 (Case 1) and 21 (Case 2) which indicate the amount of attenuation in regard to the in-band power emission level of the railway RSTT system emissions in order that they meet the EESS (passive) interference protection criteria for radiometer L-8. The two cases were examined with the railway RSTT system antenna gain in the mainlobe at 44 dBi, and the density of railway RSTT systems set at 10 and 100 in the CPR footprint, respectively. The EESS passive interference protection criteria threshold is −169.0 dBW. The calculations show that the EESS (passive) interference criteria are met with margin of 8.3 dB for Case 1 but the calculated attenuation in regard to the in-band power emission level of the railway RSTT system needed to meet the EESS (passive) interference protection criteria is 1.7 dB for Case 2.

TABLE 16

RFI from railway RSTT into EESS (passive) at 92 GHz (Case 1)
First Geometric Scenario: L-8 M/L to RSTT S/L

Case 1: Calculation of receiving power at 55-degree elevation (G_t = −10 dBi, 10 railway RSTTs in beam)		
	L8	
	Value	**dB**
RSTT transmit power (W)	0.01	–20.00
Gain_xmit (dBi)		0.00
e.i.r.p. (dBW)		–20.00
Gain_rcv (dBi)		62.40
$1/R^2$ (km)	1 114.9	–60.94
$1/f^2$ (MHz)	92 000	–99.28
L-prop (dB)		–192.66
No. of RSTTs in beam	10	10.00
Interference power (dBW)		–140.26
Interference power criteria (dBW)		–169.00
Margin (dB)		–28.74

TABLE 17

RFI from railway RSTT into EESS (passive) at 92 GHz (Case 2)
First Geometric Scenario: L-8 M/L to RSTT S/L

Case 2: Calculation of receiving power at 55-degree elevation (G_t = 14 dBi, 100 railway RSTTs in beam)		
	L8	
	Value	**dB**
RSTT transmit power (W)	0.01	–20.00
Gain_xmit (dBi)		14.00
e.i.r.p. (dBW)		–6.00
Gain_rcv (dBi)		62.40
$1/R^2$ (km)	1 114.9	–60.94
$1/f^2$ (MHz)	92 000	–99.28
L-prop (dB)		–192.66
No. of RSTTs in beam	100	20.00
Interference power (dBW)		–116.26
Interference power criteria (dBW)		–169.00
Margin (dB)		–52.74

TABLE 18

RFI from railway RSTT into EESS (passive) at 92 GHz (Case 1)
Second Geometric Scenario: L-8 S/L to RSTT S/L

Case 1: Calculation of receiving power at 90-degree elevation (G_t = 0 dBi, 10 railway RSTTs in beam)		
	L8	
	Value	**dB**
RSTT transmit power (W)	0.01	–20.00
Gain_xmit (dBi)		–10.00
e.i.r.p. (dBW)		–30.00
Gain_rcv (dBi)		–9.80
$1/R^2$ (km)	700	–56.90
$1/f^2$ (MHz)	92 000	–99.28
L-prop (dB)		–188.62
No. of RSTTs in beam	10	10.00
Interference power (dBW)		–218.42
Interference power criteria (dBW)		–169.00
Margin (dB)		49.42

TABLE 19

RFI from railway RSTT into EESS (passive) at 92 GHz (Case 2)
Second Geometric Scenario: L-8 S/L to RSTT S/L

Case 2: Calculation of receiving power at 90-degree elevation (G_t = 14 dBi, 100 railway RSTTs in beam)		
	L8	
	Value	**dB**
RSTT transmit power (W)	0.01	–20.00
Gain_xmit (dBi)		14.00
e.i.r.p. (dBW)		–6.00
Gain_rcv (dBi)		–9.80
$1/R^2$ (km)	700	–56.90
$1/f^2$ (MHz)	92 000	–99.28
L-prop (dB)		–188.62
No. of RSTTs in beam	100	20.00
Interference power (dBW)		–184.42
Interference power criteria (dBW)		–169.00
Margin (dB)		15.42

TABLE 20

**RFI from railway RSTT into EESS (passive) at 92 GHz (Case 1)
Third Geometric Scenario: L-8 S/L to RSTT M/L**

Case 1: Calculation of receiving power at 0-degree elevation (G_t = 44 dBi, 10 railway RSTTs in beam)		
	L8	
	Value	**dB**
RSTT transmit power (W)	0.01	–20.00
Gain_xmit (dBi)		44.00
e.i.r.p. (dBW)		24.00
Gain_rcv (dBi)		–9.80
$1/R^2$ (km)	3 069	–69.74
$1/f^2$ (MHz)	92 000	–99.28
L-prop (dB)		–201.46
No. of RSTTs in beam	10	10.00
Interference power (dBW)		–177.26
Interference power criteria (dBW)		–169.00
Margin (dB)		8.26

TABLE 21

**RFI from railway RSTT into EESS (passive) at 92 GHz (Case 2)
Third Geometric Scenario: L-8 S/L to RSTT M/L**

Case 2: Calculation of receiving power at 0-degree elevation (G_t = 44 dBi, 100 railway RSTTs in beam)		
	L8	
	Value	**dB**
RSTT transmit power (W)	0.01	–20.00
Gain_xmit (dBi)		44.00
e.i.r.p. (dBW)		24.00
Gain_rcv (dBi)		–9.80
$1/R^2$ (km)	3 069	–69.74
$1/f^2$ (MHz)	92 000	–99.28
L-prop (dB)		–201.46
No. of RSTTs in beam	100	20.00
Interference power (dBW)		–167.26
Interference power criteria (dBW)		–169.00
Margin (dB)		–1.74

2.2 Dynamic analysis based on interference with spacecraft orbit simulation

Calculations are performed to determine the interference from RSTT into the EESS (passive) band. The compatibility study is performed with respect to the RSTT system outlined in this Report with deployment limited to high speed rail lines in Japan. Any deployment outside Japan or deployment density changes would require the simulation to be updated to verify if co-existence is possible.

The interfering signal power level, I (dBW), received by a spaceborne radiometer from a terrestrial source is calculated from:

$$I = 10 \log P_t + G_t + G_r - (32.44 + 20 \log (f\,R)) - L_a - FDR - X_r \quad \text{(A3-2)}$$

where:

- P_t : peak terrestrial source transmitter power (W)
- G_t : terrestrial source antenna gain towards spaceborne sensor (dBi)
- G_r : spaceborne radar antenna gain towards terrestrial source (dBi)
- f : frequency (MHz)
- R : slant range between spaceborne sensor and terrestrial source (km)
- L_a : attenuation due to atmospheric absorption (dB)
- FDR : Frequency Dependent Rejection (dB)
- X_r : losses due to polarization mismatch (dB).

An assessment of the RFI expected from RSTT systems into EESS (passive) is achieved by a dynamic simulation. The analysis was conducted in which the orbit of the EESS (passive) spacecraft under investigation (i.e. the radiometers L8 and L5 described in Table 7) was dynamically simulated.

Based on time series values for the interfering signal power level, a CCDF curve will be generated in order to assess if the result exceeds the criteria defined in Recommendation ITU-R RS.2017. From Recommendation ITU-R RS.2017, the following limits should hold:

– For frequency band: 86-92 GHz, reference bandwidth: 100 MHz,
  - Maximum interference level: −169 dBW,
  - Percentage of area or time permissible interference level may be exceeded: 0.01%. The area analysed should be 2 000 000 km^2.

Recommendation ITU-R RS.1861 contains the operating characteristics for the 86-92 GHz EESS (passive).

2.2.1 Deployment of RSTT systems

With respect to the passive band, this study used the deployment over Japan and used high-speed rail data available from open source mapping software. The location data collected corresponds to the latitude and longitude of high-speed rail track locations. These locations were used as potential coordinates for RSTT stations. Deployment of the RSTT stations was achieved by activating a number of these stations corresponding to the perceived worst case as prescribed in § 6.5. The activated transceiver densities around Tokyo were provided in Table 3 along with the total length of high-speed rail in Japan, 3 418.3 km. The number of transceivers were taken from the average density shown in Table 3 multiplied by the total track length to give a total of 8 648 active stations. The active stations were chosen from a larger pool with a uniform random probability. A higher density of RSTT stations is concentrated in urban areas as a result of the density of track locations in these areas. The activated RSTT stations were randomly selected for each time step of the simulation to achieve a Monte Carlo approach to the simulation. An example of the full deployment is shown in Fig. 16 along with a blue rectangle which represents the test measurement area, encompassing Japan, of 2 000 000 km^2 specified by Recommendation ITU-R RS.2017.

FIGURE 16

Two million km^2 measurement area of interest over Japan

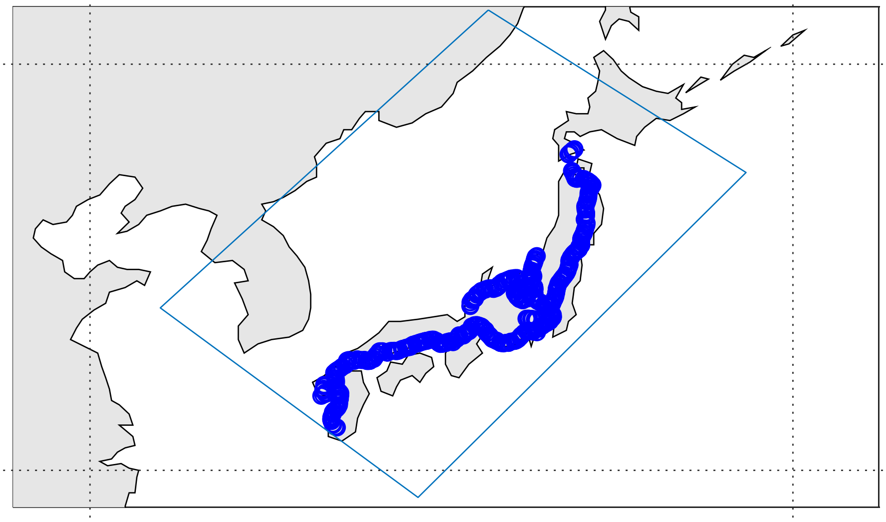

2.2.2 Characteristics of RSTT systems

The description of the RSTT parameters used for this analysis is given in Table 22. The received interference is calculated based on the aggregate power received by EESS (passive) from all RSTT nodes within a possible line of sight.

TABLE 22

Assumed characteristics of RSTT system networks

Parameter	Value
In Band RSTT transmit power	−20 dBW/100 MHz
Elevation angle (degree)	0
Azimuth	Fixed Towards next element in line
Transmit height (m)	4

The RSTT system antenna radiation pattern at 96 GHz from Annex 1 was used to construct an empirical function used in the analysis. This analysis considers an RSTT antenna elevation angle of zero degrees for all antennas, further study may be needed to incorporate antenna elevation based on track gradient as outlined in § 6.6.

2.2.3 Characteristics of Earth exploration-satellite service (passive) system

2.2.3.1 Earth exploration-satellite service (passive) characteristics

In the 86-92 GHz band there currently operate two main types of EESS (passive) sensor, the conical scan and mechanical nadir scan sensors. EESS (passive) sensors L8 and L5 were simulated in this this study to verify compatibly with both a conical scan and mechanical nadir scan sensor. The operating parameters of the L8 and L5 sensors are such that they will receive a higher power from the RSTT deployment for their respected scan types. The L8 sensor in this incidence is the best model to protect the EESS (passive) service for present and future missions. EESS (passive) satellite orbit parameters and technical and operational characteristics of Sensors L8 and L5 are shown in Recommendation ITU-R RS.1861, which operates in the 86-92 GHz band. EESS (passive) receive filters frequency response is assumed to provide sufficient attenuation outside of the 86-92 GHz band to allow limiting the sharing study within the 86-92 GHz band. Recommendation ITU-R RS.1813-1 was used to generate the antenna patterns for the passive sensors of the study. The antenna gain plots are shown in Fig. 17 with gains normalized to 0 dBi.

FIGURE 17

EESS (passive) sensor l8 and Sensor L5 gain

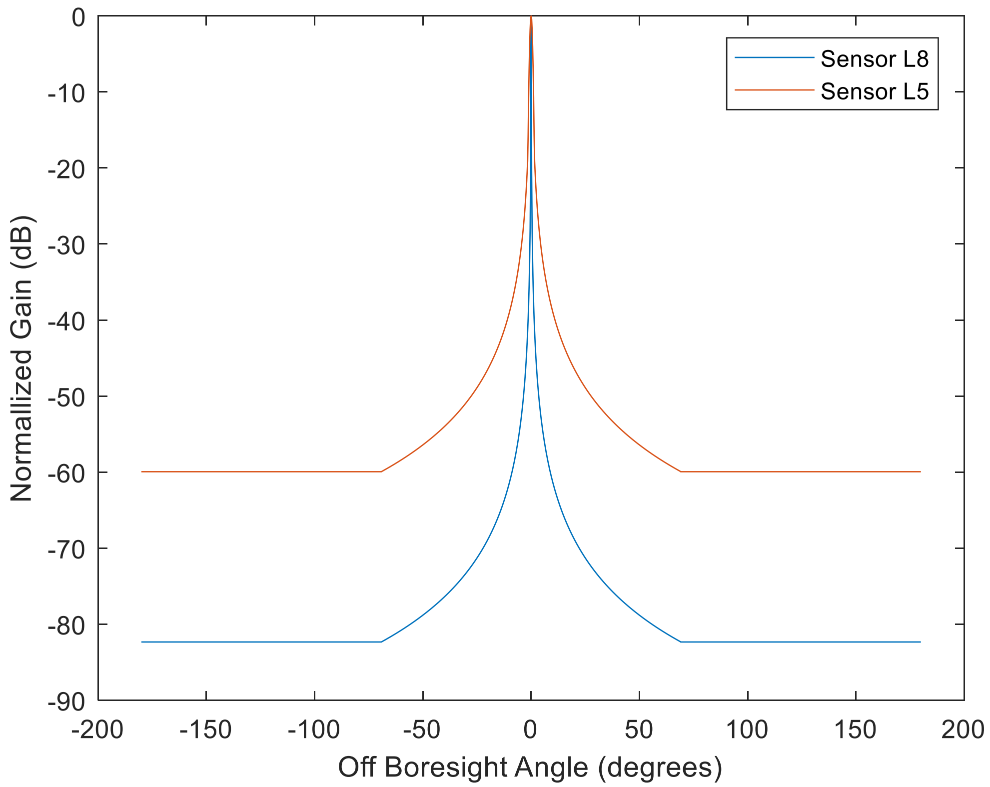

2.2.3.2 Earth exploration-satellite service (passive) sensor area of interest test cases

The 86-92 GHz EESS (passive) analysis of this study will focus on current high-speed rail lines inside Japan within the measurement area of interest. If the number of forecasted activation densities changes or if RSTT is expanded to other rail lines or future rail lines the simulation will need updated to verify co-existence.

2.2.4 Simulation parameters and results

2.2.4.1 General simulation parameters

For the 86-92 GHz band, Recommendation ITU-R RS.2017 prescribes interference shall not exceed the power spectral density of −169 dBW/100 MHz over any part of the band for .01% of the time. A simulation frequency of 91 950 MHz, 50 MHz from the band edge, with a 100 MHz bandwidth was chosen to be in line with the EESS (passive) protection criteria of −169 dBW/100 MHz. Analysis was done along the band edge to determine the level of unwanted emissions into the EESS (passive) band. Table 23 gives the rest simulation parameters that were assumed for this simulation.

TABLE 23

General simulation parameters

Parameter	Value
Simulation frequency (MHz)	91 950
Duration (days)	16, 29
Time step (s)	0.05×π
Atmospheric losses	P.676
Polarization losses (dB)	3
FDR (dB)	34
EESS (passive) band power (dBW/100 MHz)	−54

The simulation was run for a 16- or 29-day duration with a 0.05 × π second time step to encompass the repeat period of the sensor L8 or L5 respectively. This duration and time step included an appropriate amount of sample points to achieve statistical significance of results. Atmospheric losses (L_a) were calculated using Recommendation ITU-R P.676. The irrational time step of 0.05 × π was chosen to create a random non-uniform distribution of the EESS locations and azimuth pointing angles during satellite orbit within the simulation run time. This analysis assumes the band edge power −40 dBm/3 MHz at 92 GHz, from the measured spectrum as described in § 7.1 and Fig. 10. This equates to −54 dBW/100 MHz if a flat power density is assumed in the 91.90 to 92 GHz EESS (passive) range. Thus, an unwanted emission power level of −54 dBW in 100 MHz was assumed in the simulations, demonstrating an FDR of 34 dB with transmit power of −20 dBW/100 MHz. If the FDR is lower than the presumed value, the simulation and co-existence may have to be revaluated.

2.2.4.2 Simulation results

The dynamic analysis was run using the general simulation parameters found in Table 23. Only the satellite locations of the where the main beam of the satellite were pointing inside the measurement area of interest were retained for analysis, and the ground track of the EESS (passive) satellites over the measurement area of interest in shown in Figs 18 and 19. The aggregate interference levels for each time step in the simulation were calculated and used to create a complementary cumulative distribution function (CCDF), Figs 20 and 21. The CCDF below demonstrates what percentage of the time steps the aggregate interference was above the specified level on the x-axis. The EESS (passive) protection criteria for the 86-92 GHz band specifies that aggregate interference values of −169 dBW/100 MHz may occur in no more than 0.01% of the time steps. The results of the simulation, for Sensor L8, show a received aggregate interference power of greater than or equal to −179.5 dBW/100 MHz for 0.01% of the time for a 2.53 active stations per kilometre. The results of the simulation, for Sensor L5, show a received aggregate interference power of greater than or equal to −187 dBW/100 MHz for 0.01% of the time for a 2.53 active stations per kilometre. Figures 22 and 23 offer a snapshot of the EESS (passive) Sensor L8's dynamics at a discrete time step, showing the off-boresight angle and corresponding gain, respectively.

FIGURE 18

EESS (passive) Sensor I8 orbit over MAI

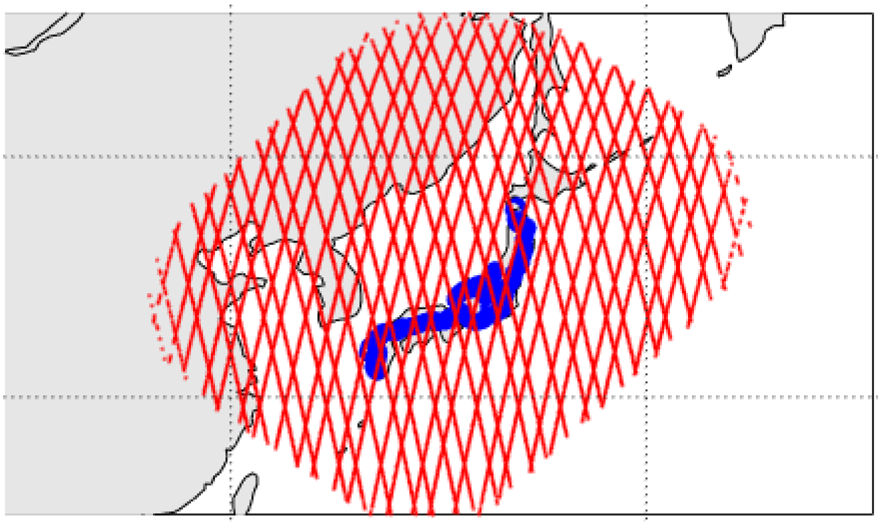

FIGURE 19

EESS (passive) Sensor I5 orbit over MAI

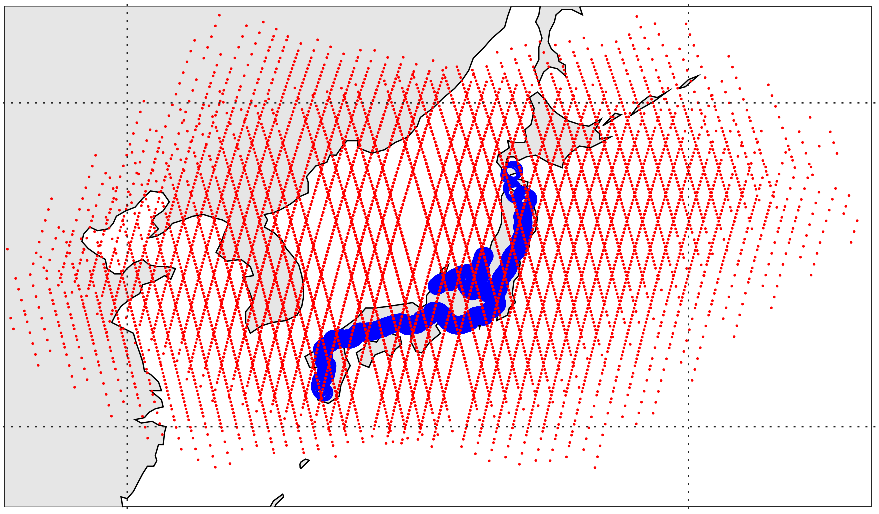

FIGURE 20

EESS (passive) Sensor I8 CCDF

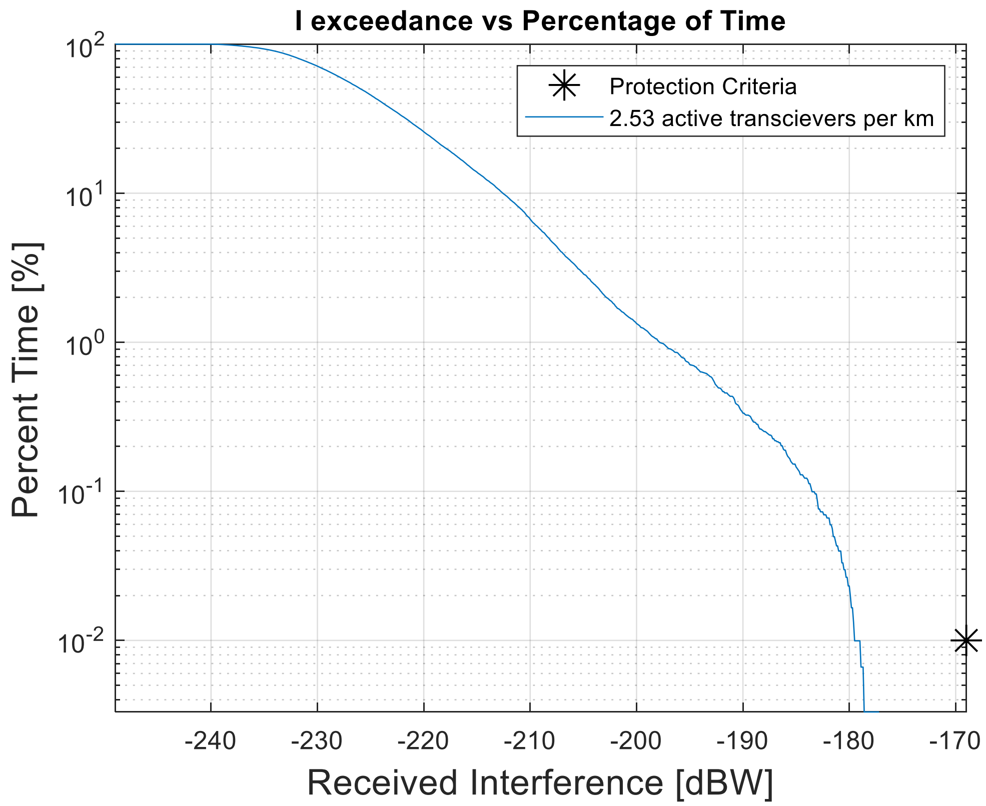

FIGURE 21

EESS (passive) Sensor I5 CCDF

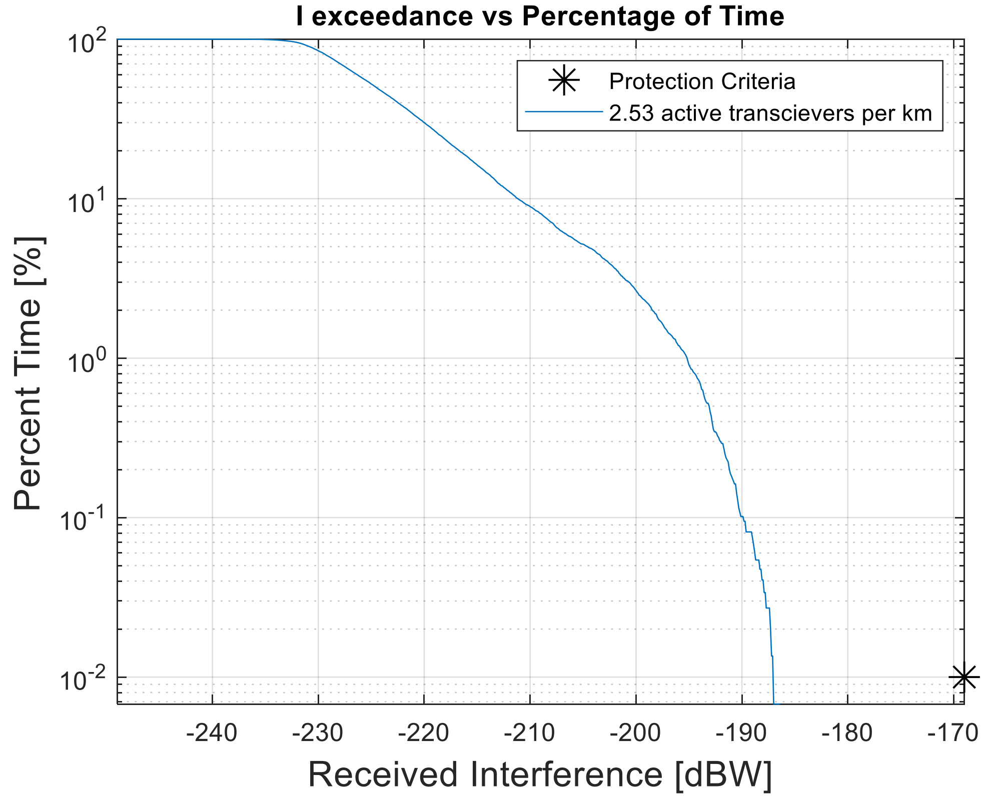

FIGURE 22

Example of EESS (passive) sensor L8 off-boresight Angle at a discrete time step, EESS (passive) main beam intersection with Earth noted with (*)

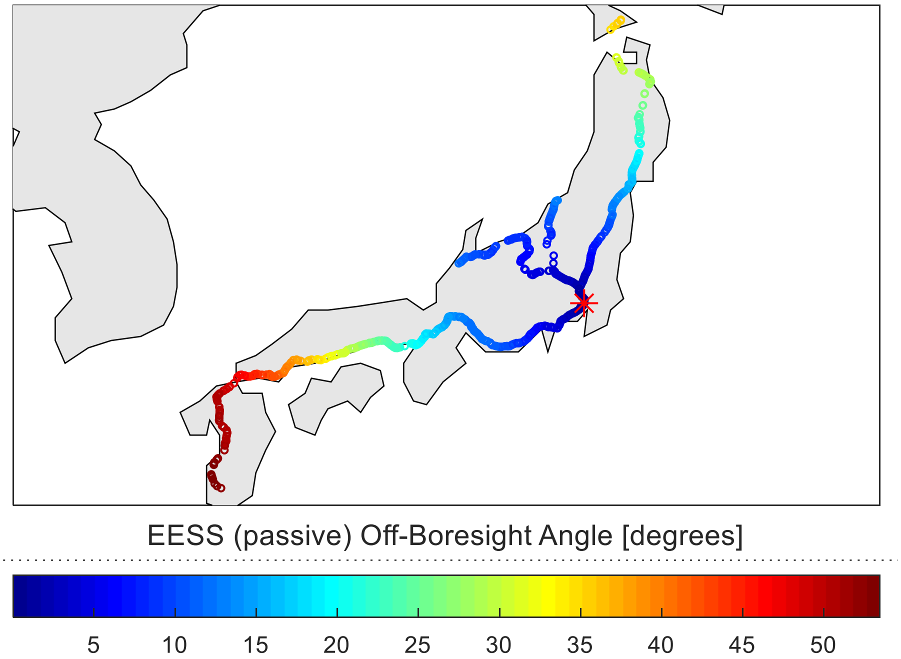

FIGURE 23

Example of EESS (passive) Sensor L8 GAIN towards EACH RSTT Point at a discrete time step, EESS (passive) main beam intersection with Earth noted with (*)

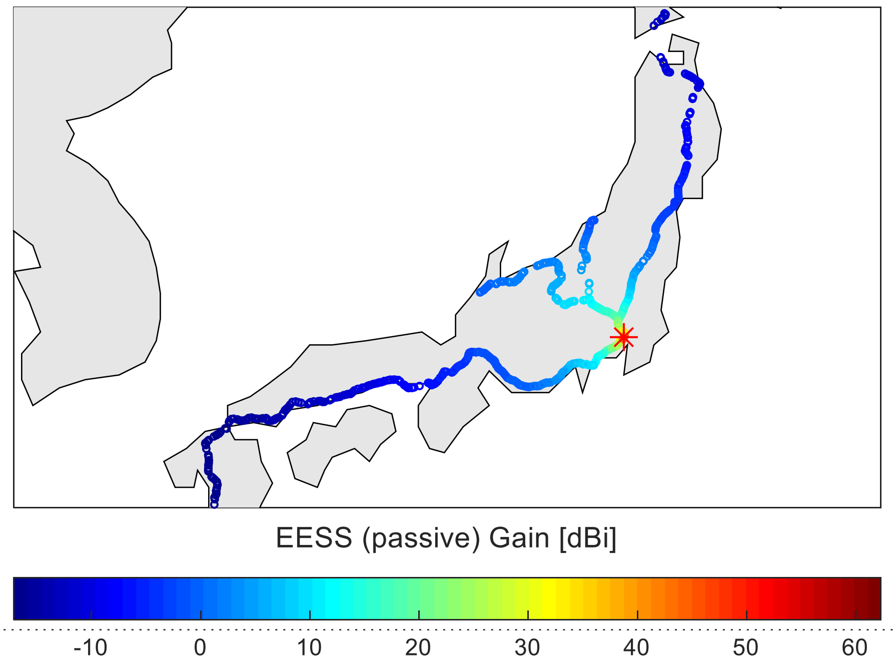

3 Summary

Results of the static calculations show for the three different geometrical interaction scenarios described involving antenna beam coupling between railway RSTT systems and spaceborne radiometers, the RFI levels at the radiometer L8 are highest for the geometrical situation of coupling between the mainlobe of the radiometer L8 antenna and the sidelobes of the railway RSTT system antenna. With the second geometrical scenario where there is coupling of the sidelobes of both the radiometer L8 antenna and the railway RSTT system antenna; the RFI levels are lower than for the first geometric scenario. In the third geometrical scenario where coupling between the mainbeam of the railway RSTT system antenna and the radiometer L8 antenna sidelobes with the radiometer L8 satellite on the horizon with respect to the railway RSTT systems occurs, the interference was lower than the first geometric scenario as well. Two cases of railway RSTT deployment and their interference impact to radiometer L8 were analysed to arrive at a preliminary calculation of attenuation in regard to in-band emission levels of railway RSTT systems. The two cases consider the railway RSTT antenna gain in the sidelobes at the level in Fig. 2 for the appropriate elevation angle and a higher level estimated due to irregularities in the trainside area, and the density of railway RSTT systems at 10 and 100 in the footprint of the CPR-L1 sensor. For the first geometric scenario, in order to meet the EESS (passive) Recommendation ITU-R RS.2017 protection criteria for spaceborne radiometers, railway RSTT system in-band emission levels would have to be attenuated 28.7 dB when considering Case 1 and 52.7 dB when considering Case 2 at the band edges adjoining the EESS (passive) band 86.0-92.0 GHz.

Results of the dynamic simulation between the assumed deployment of RSTT and EESS (passive) show a margin of 4 to 13 dB with respect to the EESS (passive) protection criteria. Recommendation ITU-R RS.2017 states that in the 86-92 GHz band interference values of −169 dBW/100 MHz may occur in no more than 0.01% of the time steps. The results of the simulation, for Sensor L8, show a received aggregate interference power of greater than or equal to −179.5 dBW/100 MHz for 0.01% of the time for a 2.53 active stations per kilometre. The results of the simulation, for Sensor L5, show a received aggregate interference power of greater than or equal to −187 dBW/100 MHz for 0.01% of the time for a 2.53 active stations per kilometre.

Annex 4

Sharing studies between RAS and RSTT systems in the frequency range 92-109.5 GHz

The protection criteria for radio astronomical observations are given in Recommendations ITU-R RA.769 and ITU-R RA.1513. More precisely, an interpolation from the interference threshold levels given for the frequency bands listed in Recommendation ITU-R RA.769 provides the following threshold spectral power flux densities for continuum and spectral line observations in the frequency range 92-109.5 GHz. According to Recommendation ITU-R RA.1513, interference from any one network should not exceed these thresholds for more than 2% of time.

TABLE 24

Interference threshold level of radio astronomical observations

Frequency band (GHz)	Threshold interference level – Input power (dBm)	
	Continuum observations (8 GHz bandwidth)	Spectral line observations (1 MHz bandwidth)
92-109.5	–159	–179

The bands 92-94 GHz, 94.1-100 GHz and 102-109.5 GHz are allocated on an equal primary basis to the mobile service and radio astronomy service including other radiocommunication services in all three Regions. The protection criterion used is derived from Recommendation ITU-R RA.769-2. The received power level at the radiometer is calculated by the following equation:

$$P_{769} = Pt + G - Loss - J(\nu)$$

$$= Pt + G - (92.5 + 20 * \log(f) + 20 * \log(d) + Ag) - J(\nu)$$

where:

Pt : transmission power of on-board equipment

G : antenna gain

d : separation distance

$Loss$: propagation loss given by Recommendation ITU-R P.452-16

$J(\nu)$: knife-edge diffraction loss given by Recommendation ITU-R P.452-16.

$$Ag = (\gamma_o + \gamma_w(\rho))d$$

where:

Ag : total gaseous absorption (dB)

$\gamma_o + \gamma_w(\rho)$: specific attenuation due to dry air and water vapour, respectively, and are found from the equations in Recommendation ITU-R P.676

ρ : water vapour density:

$$\rho = 7.5 + 2.5\omega \quad \text{g/m}^3$$

ω : fraction of the total path over water.

A4.1 Impact to Nobeyama Radio Observatory from RSTT transmitter in Kokubunji area

The separation distance which satisfies with the requirement of protection level is calculated from the above equation. The line-of-sight scenario from the on-board equipment to the radio astronomy antenna is also evaluated as the worst-case scenario in this case. Figure 24 shows the topographic profile between Nobeyama Radio Observatory and Kokubunji where NICT is located. The distance is 87.8 km, and the altitudes of each location are about 1 350 m and 95 m, respectively. As the first calculation example, the single knife-edge diffraction loss caused by the highest mountain (2 418 m) is calculated and its value of 64.5 dB is obtained. Table 25 summarizes the initial result of received power level at Nobeyama Radio Observatory. For the first geometric study, the received power at RAS site is 0.1-dB larger and 64-dB lower than the interference threshold level in line-of-sight and non-line-of-sight propagation paths, respectively.

FIGURE 24

Topographic profile between Nobeyama Radio Observatory and Kokubunji

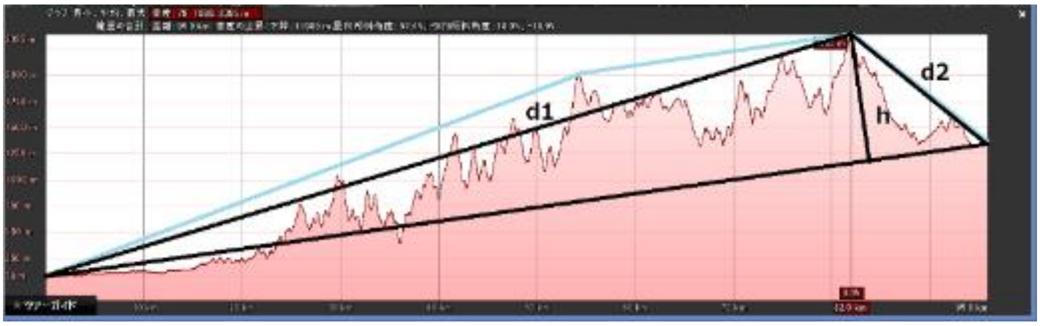

TABLE 25

Received power level at Nobeyama Radio Observatory

Parameters	Value	Note
RSTT transmitting power/channel (mW)	10	
RSTT antenna gain (dB)	42	
Centre frequency (GHz)	92.5	
Distance between RSTT transmitter and RAS antenna (km)	87.8	
Gaseous absorption (dB	34.2	
Knife-edge diffraction loss (dB)	64.5	Non-line-of-sight
Channel bandwidth (MHz)	400	
Received power reduction by 1 MHz	–26	
Received power level at RAS site (dBm)	–243.4	Non-line-of-sight
Received power level at RAS site (dBm)	–178.9	Line-of-sight

A4.2 Impact to Nobeyama Radio Observatory from RSTT transmitter in Saku area

Figure 25 shows a map in the Saku area where the Nobeyama Radio Observatory is located. Hokuriku super-express line is shown by the blue-white coloured line, however there are many tunnels in this area. The topographic profiles of three links 1, 2, 3, 4, 5 and 6 from Nobeyama Radio Observatory to Hokuriku super-express line are shown in Fig. 26. It should be noted that no line-of-sight links between Nobeyama Radio Observatory and Hokuriku super-express line are observed in Saku area.

FIGURE 25

Locations of the Nobeyama 45-m telescope and Sakudaira and Ueda stations of Hokuriku super-express line in Saku area

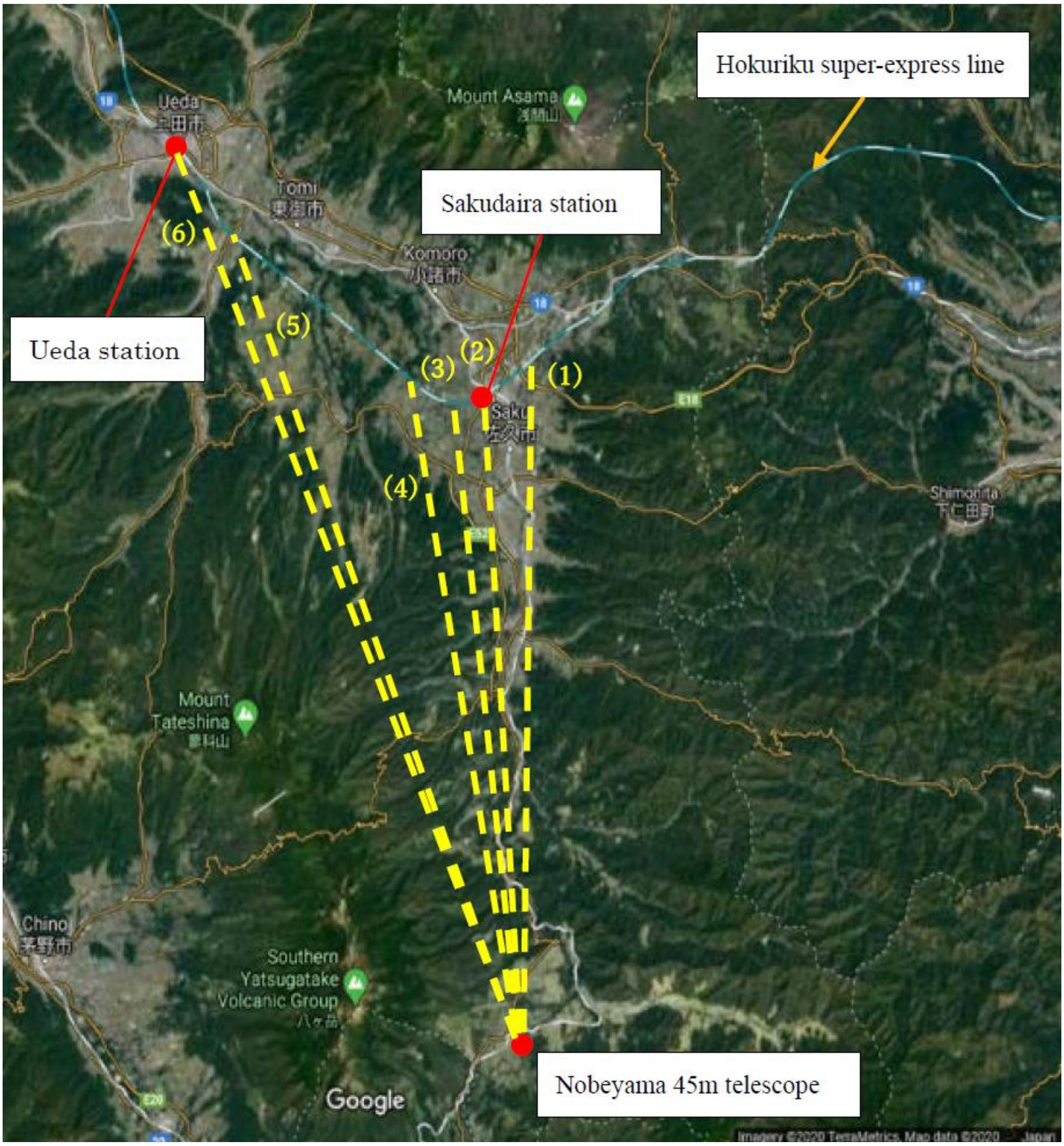

FIGURE 26

Topographic profiles between Nobeyama Radio Observatory and Hokuriku super-express line

(a) Link 1 where d1 = 34029.1 m, d2 = 4805.2 m, h = 36.1 m and azimuth angle = 49 degrees

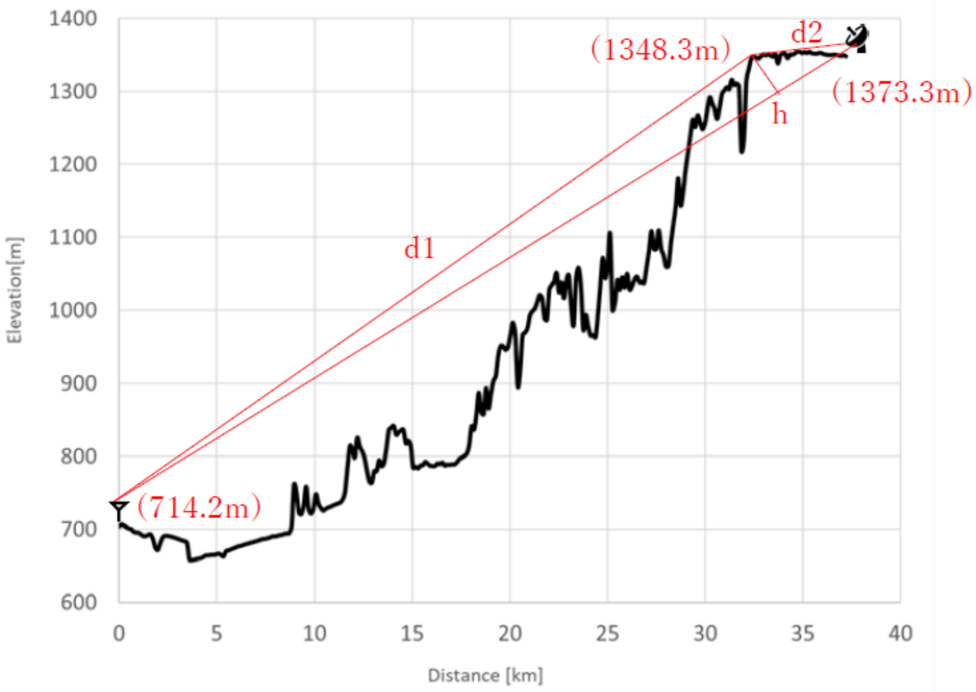

(b) Link 2 where d1 = 32485.2 m, d2 = 4729.1 m, h = 58.8 m and azimuth angle = 64 degrees

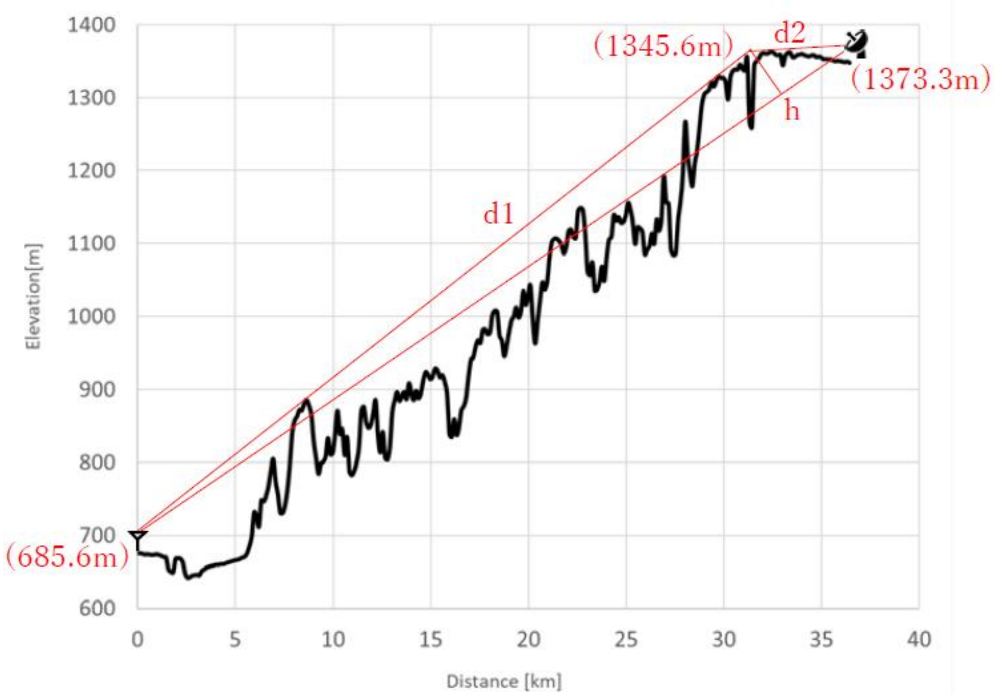

(c) Link 3 where d1 = 3 0821.1 m, d2 = 5 603.1 m, h = 78.2 m and azimuth angle = 90 degrees

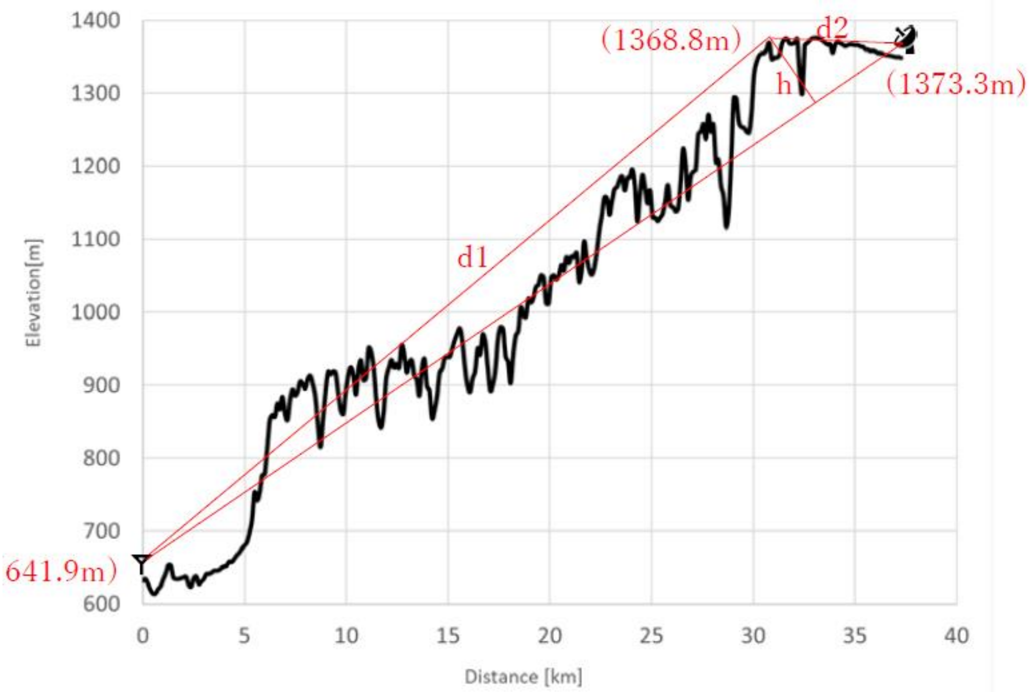

(d) Link 4 where d1 = 3 0786.6 m, d2 = 6 480.0 m, h = 122.8 m and azimuth angle = 54 degrees

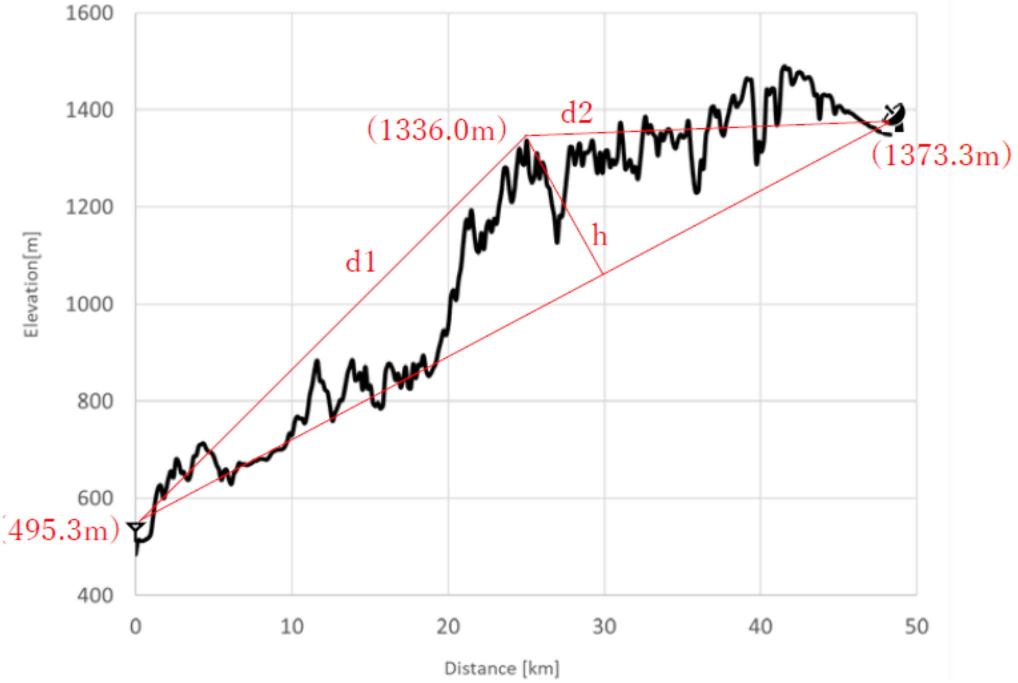

(e) Link 5 where d1 = 25043.1 m, d2 = 23253.0 m, h = 385.5 m and azimuth angle = 36 degrees

(f) Link 6 where d1 = 2 8178.7 m, d2 = 16658.4 m, d3 = 6 527.1 m, h1 = 264.7 m, h2 = 118.9 m and azimuth angle = 0 degree

Table 26 summarizes the received power level at Nobeyama Radio Observatory using the terrain profile parameters depicted in Fig. 26. The received power level of the non-line-of-sight link is much smaller than the threshold interference level of −179 dBm/MHz. The received power level of the line-of-sight link is also calculated for reference. The worst-case scenario where RSTT transmitter faces to Nobeyama Radio Observatory whose azimuth angle is equal to 0 degree and antenna gain 42 dBi specified in Table 6 in the main body of the text corresponds to the link 6. However, due to rugged terrain around Hokuriku super-express line in Saku area, it is difficult to provide the line-of-sight link in this area. In this calculation, RSTT antenna gain is adjusted according to the azimuth angle to Nobeyama Radio Observatory and the elevation angle of RSTT antenna is assumed to be 0 degree.

TABLE 26

Received power level at Nobeyama Radio Observatory from RSTT transmitter of Hokuriku super-express line

Link	Antenna gain taking into account azimuth angle to Nobeyama Radio Observatory (dBi)	Non-line-of-sight received power level (dBm/MHz)	Line-of-sight received power level for reference (dBm/MHz)
1	−3	−233.9	−198.2
2	−10	−244.2	−204.2
3	−15	−250.5	−208.6
4	−10	−249.5	−204.2
5	0	−252.6	−200.9
6	42	−256.1	−160.6

Annex 5

Frequency arrangement of 100-GHz RSTT

TABLE 27

List of centre frequencies and bandwidth of each channel, and each guard band frequencies

Channel number	Centre frequency (GHz)	Bandwidth (MHz)	Remark
			Guard band: 92.0-92.2 GHz
1	92.4	400	
2	92.8	400	
3	93.2	400	
4	93.6	400	
			Guard band: 93.8-94.0 GHz, 94.1-94.5 GHz
5	94.7	400	
6	95.1	400	

TABLE 27 (*end*)

Channel number	**Centre frequency (GHz)**	**Bandwidth (MHz)**	**Remark**
7	95.5	400	
8	95.9	400	
9	96.3	400	
10	96.7	400	
11	97.1	400	
12	97.5	400	
13	97.9	400	
14	98.3	400	
15	98.7	400	
16	99.1	400	
17	99.5	400	
			Guard band: 99.7-100.0 GHz, 102.0-102.3 GHz
18	102.5	400	
19	102.9	400	
20	103.3	400	
21	103.7	400	
22	104.1	400	
23	104.5	400	
24	104.9	400	
25	105.3	400	
26	105.7	400	
27	106.1	400	
28	106.5	400	
29	106.9	400	
30	107.3	400	
31	107.7	400	
32	108.1	400	
33	108.5	400	
34	108.9	400	
			Guard band: 109.1-109.5 GHz